RW_SEM

Appendices

Analysis of the tide on the Hooghly River; Calibration and alteration of a model computing the vertical distribution of the suspended sediment under non-permanent flow conditions

June 1992

J. de Vletter

TU Delft

Delft University of Technology

Faculty of Civil Engineering
Hydraulic and Geotechnical Engineering Division
Hydraulic Engineering Group

Appendices

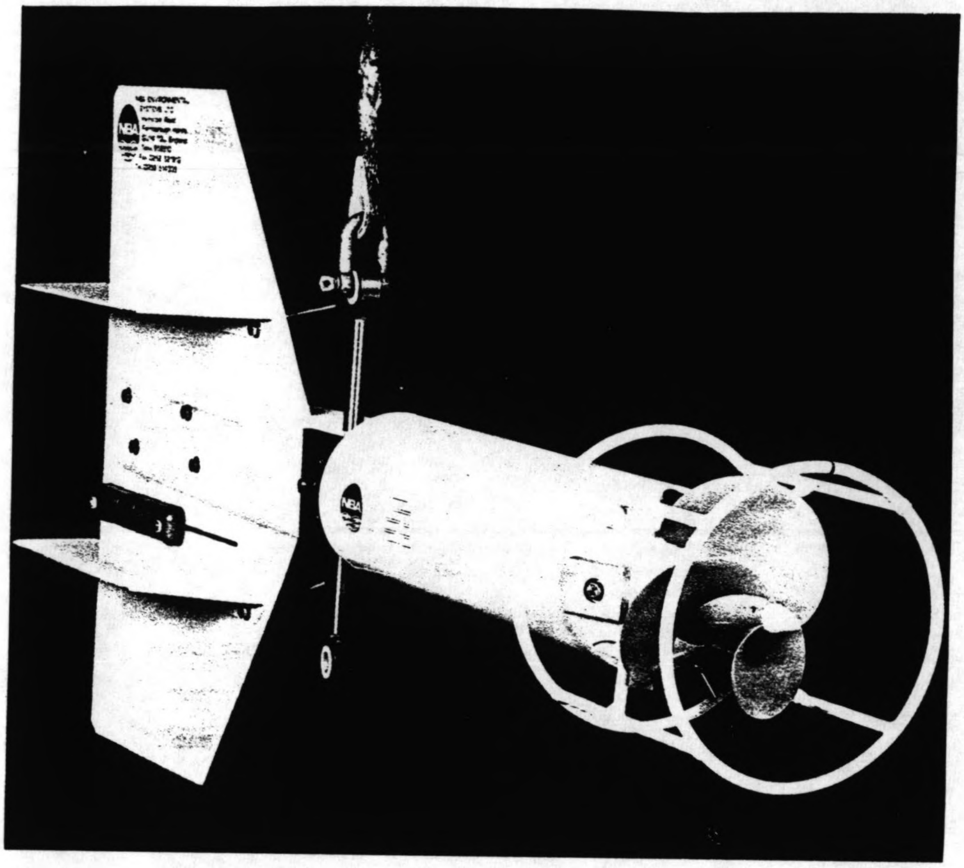

Figure 1.1

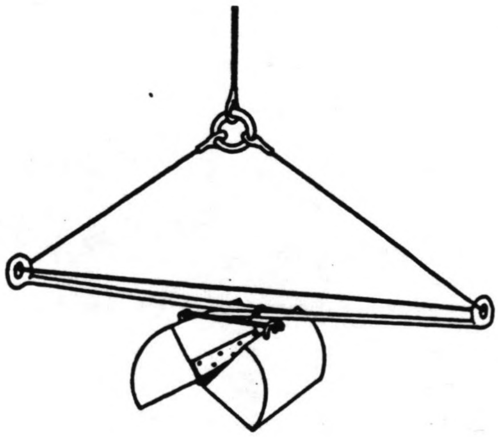

Figure 1.2

Figure 1.3

Appendix 1

Description of the instruments

The magnitude of the flow velocity was measured by the velocity meter, which counts the rotations of the impeller. Several devices are fitted in the meter, such as a magnetic compass to determine the velocity direction (average and instantaneous).
A piezo resistive transducer measures the pressure of the water head of the velocity meter. The meter itself consists of a case, containing the electronic instruments, and a tail, to keep the meter in the water in a horizontal position. The temperature of the water can also be measured. This information is put on a cartridge for every (pre-adjusted) interrogation time. The information can be read off by a computer. The meter is suspended on a rope in the water from a ship or pontoon. See ***figure 1.1***.

On the survey boat an echo sounder was installed, which registers the depth on a roll of paper. It is able to measure is a minimum depth of two meters, which is just about the draught of the ship.

A Van Veen grab can be used to take bottom samples. This is a grab that can be fixed in an open position by a pin which is removed when the grab touches the bottom. Then the grab closes and can be pulled up by the rope. See ***figure 1.2***.

The density of the water samples can be measured by using a density float (see ***figure 1.3***). After being put in the water the density can be read off on the float at the water surface.

A Niskin bottle consists of a cylinder and two stops at both ends. These stops are connected to each other through the cylinder by an elastic band. The stops are drawn from the ends of the cylinder by putting the loops of the small ropes on the stops behind a catch. See ***figure 1.4***. The Niskin bottle is suspended in the water on a rope.
When the Niskin bottle is in position, the catch can be triggered off by dropping a trigger weight along the rope. This weight falls on the trigger, the catch opens and the stops close the Niskin bottle. Next, the Niskin bottle is pulled out of the water and by opening a small tap, the sample can be poured into an empty bottle.

The positioning of the ship can be determined by several systems such as the Motorola and Syledis system. The Motorola system was preferred by the Dutch surveyors, because the Syledis system is less accurate. The latter operates on beacons, which are situated at long distances from each other resulting in the interpolation being less accurate. Moreover, the position of these beacons cannot be accurately determined because of errors in the interpretation of the receipt of the signals.

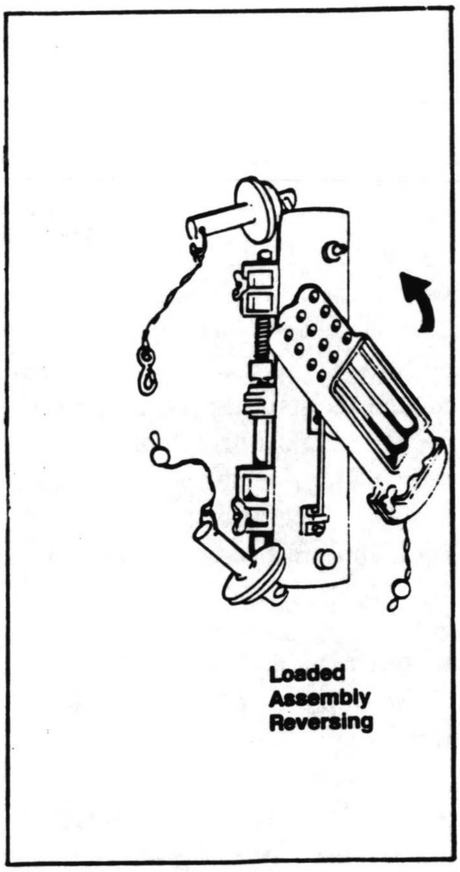

Figure 1.4

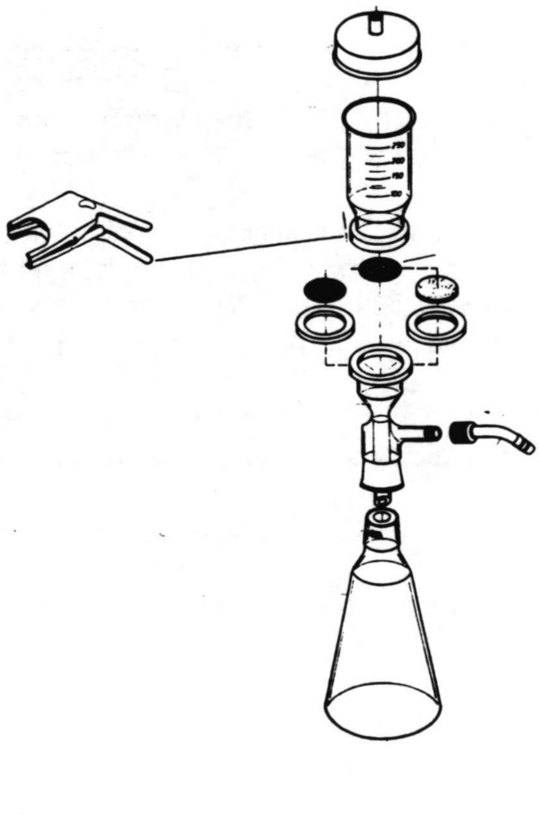

Figure 1.5

The beacons of the Motorola system were placed by the surveyors themselves during the first campaign. However, the beacons were removed afterwards and could therefore not be used for the second campaign. During the second campaign it was possible to borrow a Syledis set from the Calcutta Port Trust.

Description of the filtration method

The filtration instruments were set up as follows (see ***figure 1.5***): a bottomless graduated glass is placed on a filter, which lies on a disk of porous stone. Underneath this stone an Erlenmeyer flask with rubber stop is situated. A rubber seal is put on top of the graduated glass to avoid dust falling in.

Before filtration, the filter is weighed on a balance (accuracy of 0.1 mg). This weight is registered. Next, the bottle is shaken and a certain amount of water is poured out, usually 100 ml. This water is poured into the graduated glass. Now the water is able to leak through the filter and the porous stone into the Erlenmeyer flask. The process is stimulated by creating a vacuum in the flask. This is performed by a small pump. The filter catches the sediment and the water leaks into the Erlenmeyer flask, which is regularly emptied.
After filtration, the filter is put in a Petri dish, which is put in the oven. When the filters are dry, they are weighed again. Now the concentration can be calculated.

Appendix 2.1

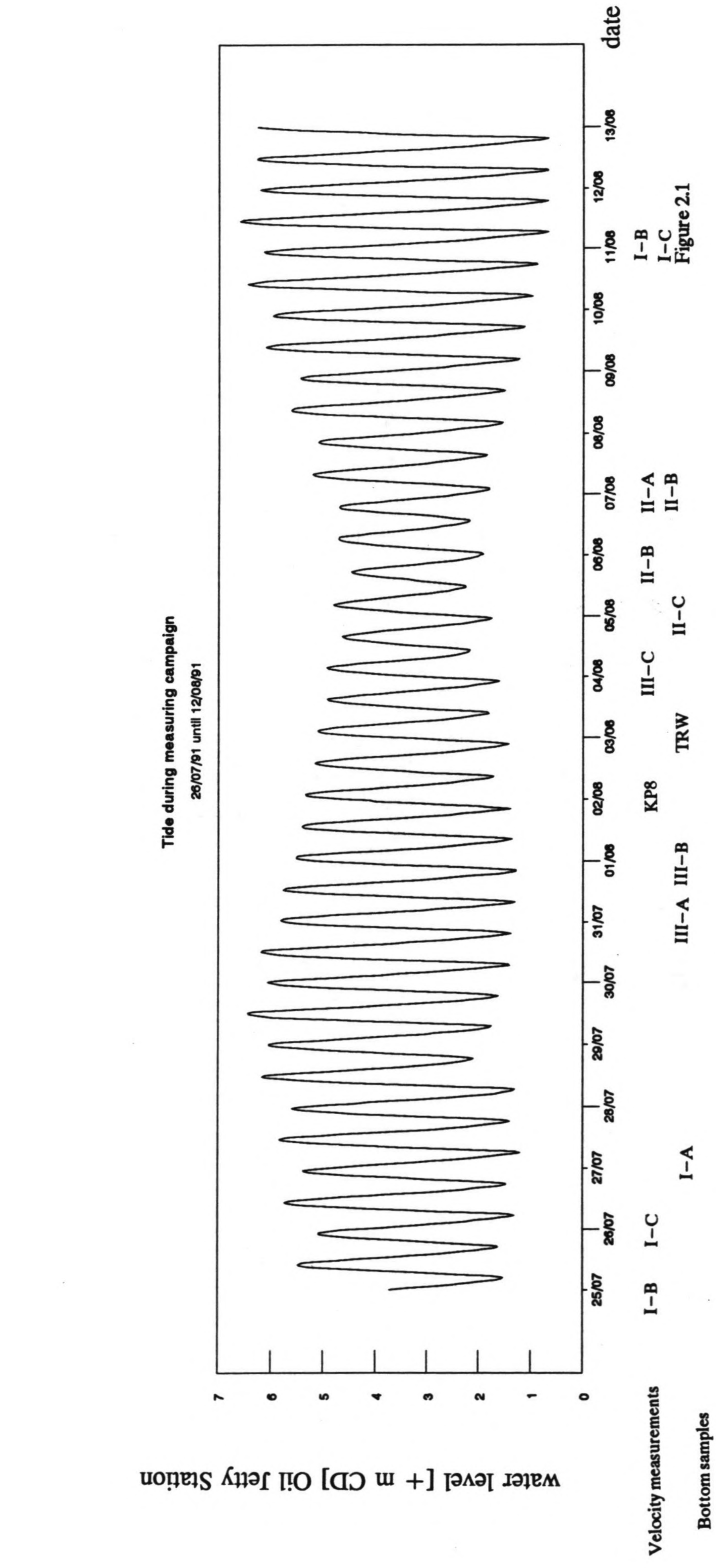

Figure 2.1

I–A
27/07/91

Figure 2.2.1.1

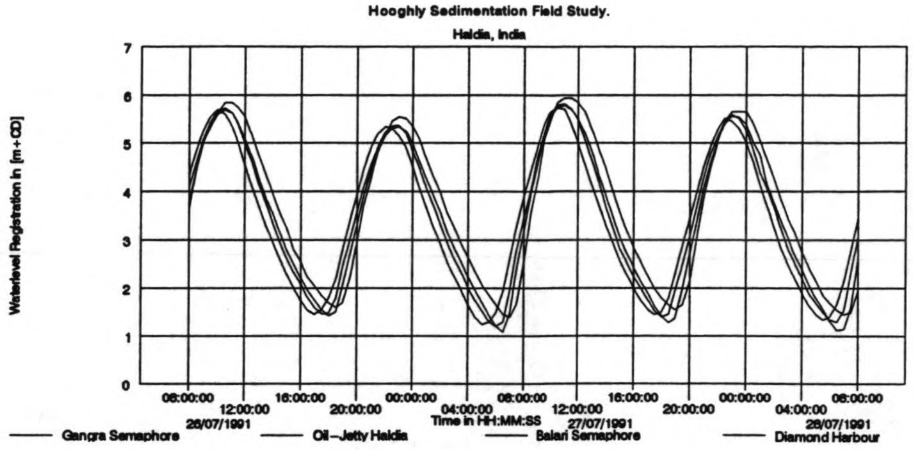

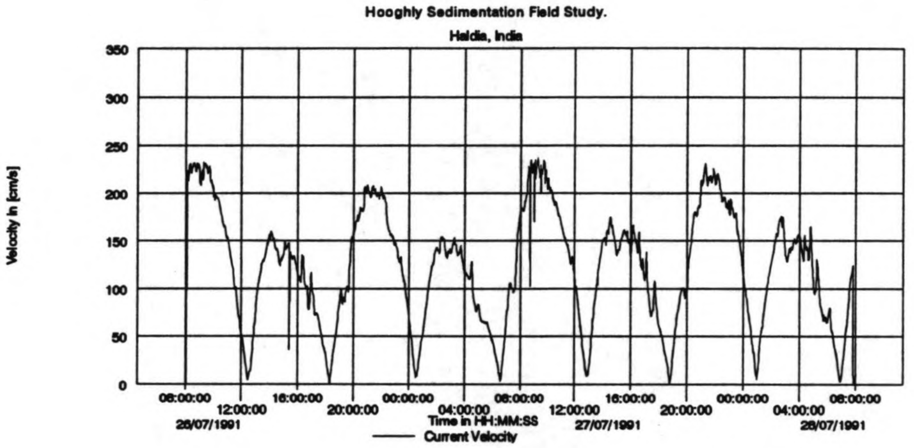

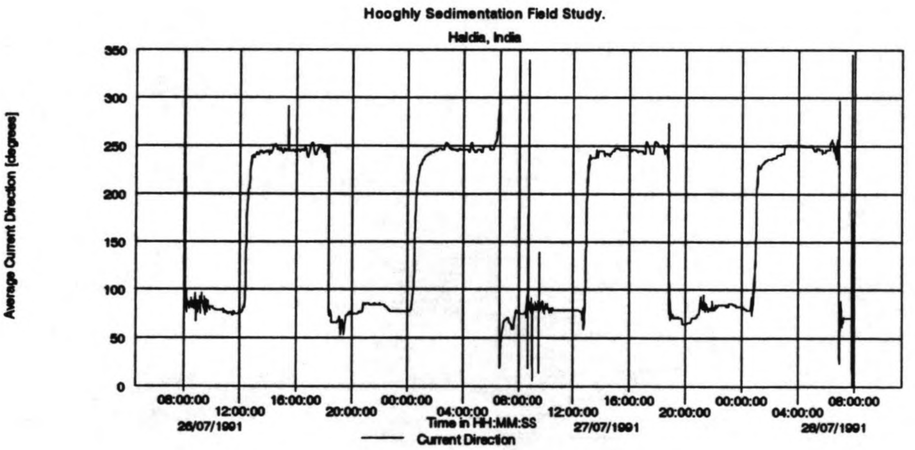

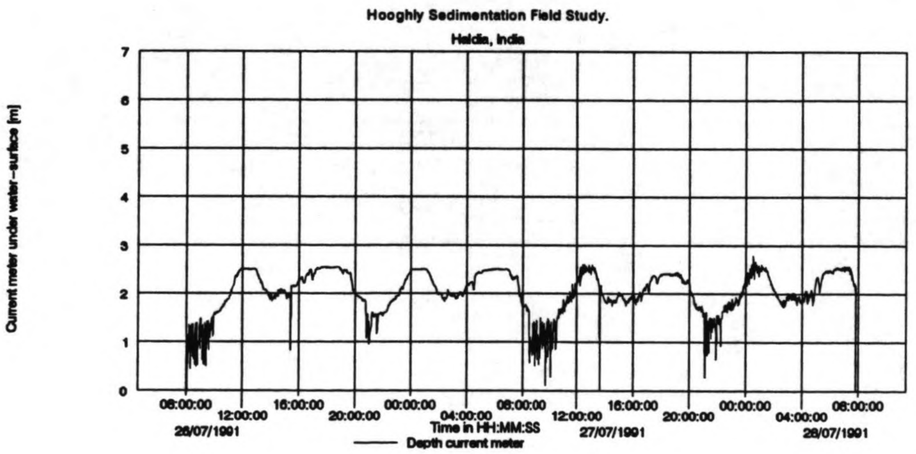

II–A
07/08/91

Figure 2.2.1.2

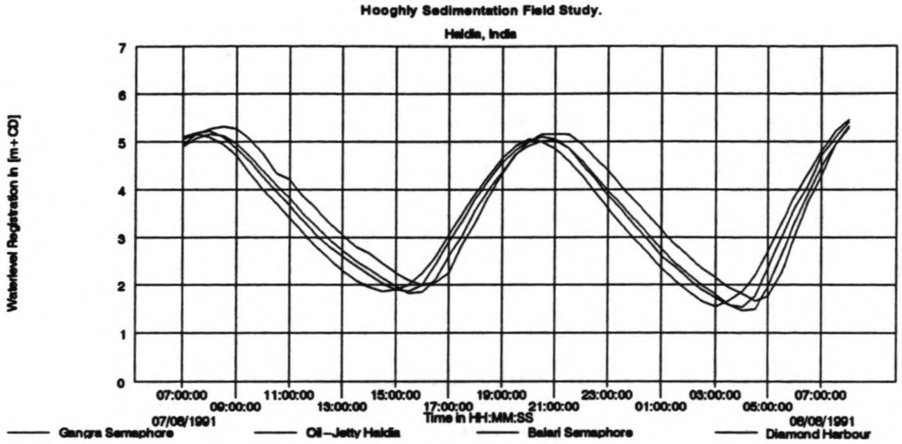

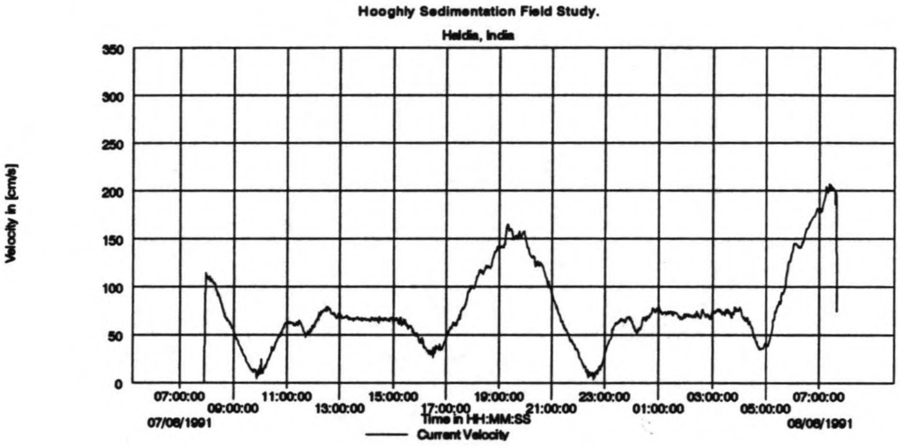

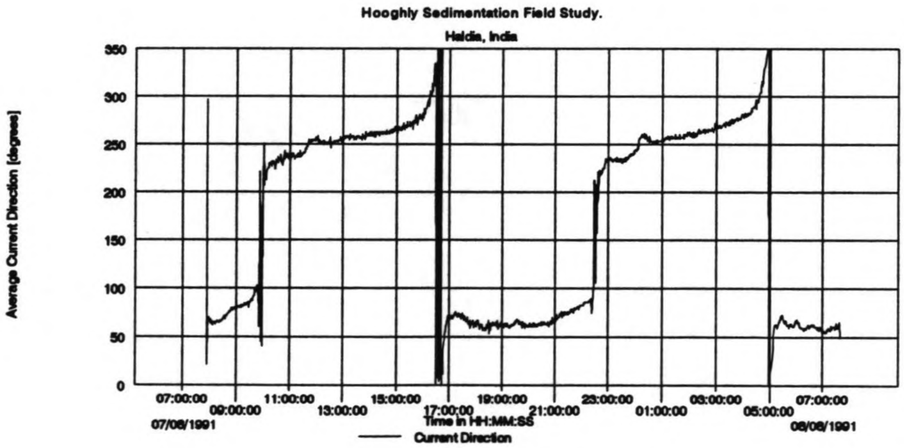

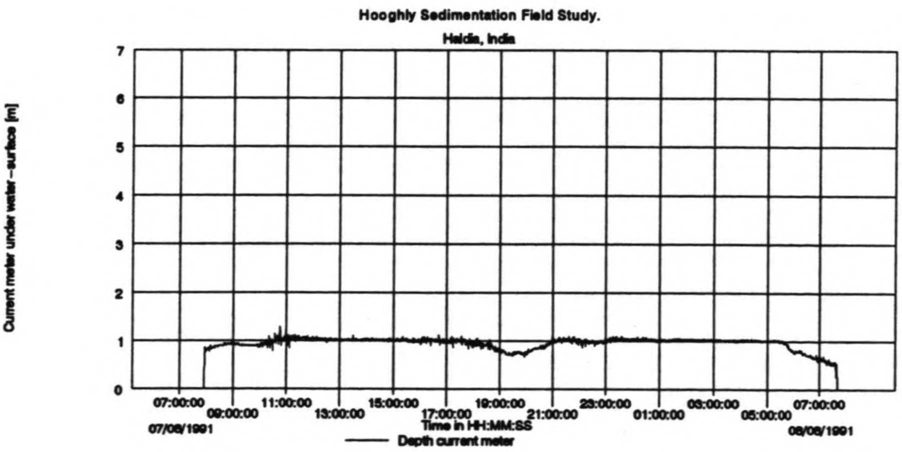

III-B
01/08/91

Figure 2.2.1.3

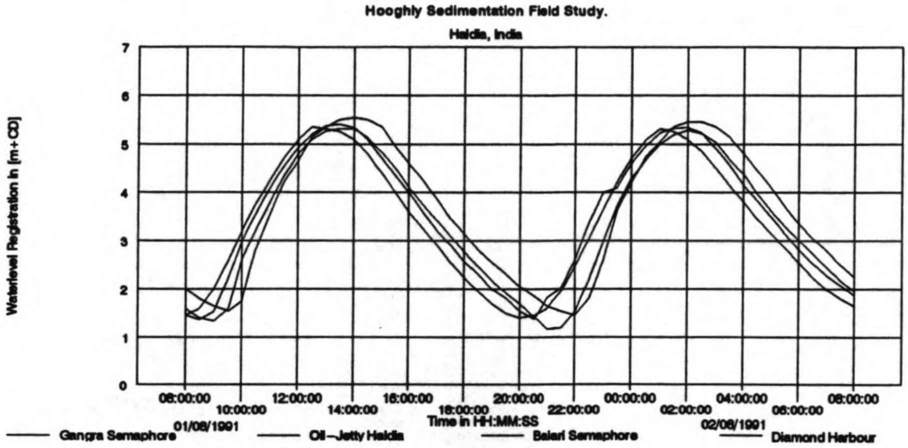

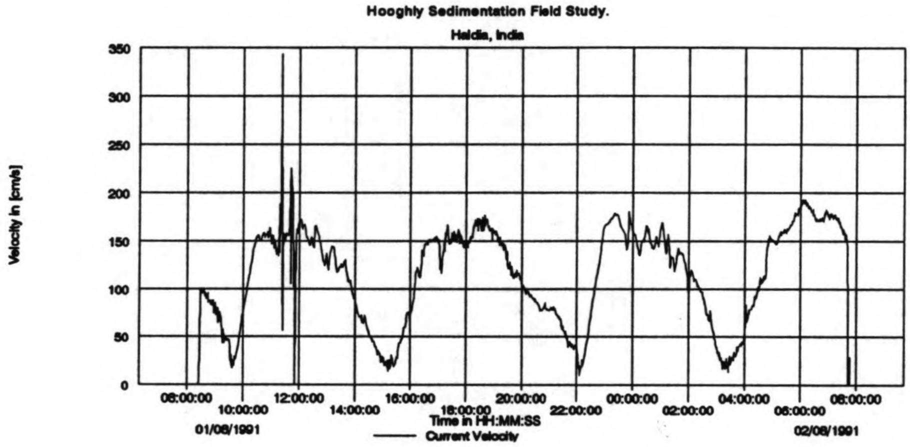

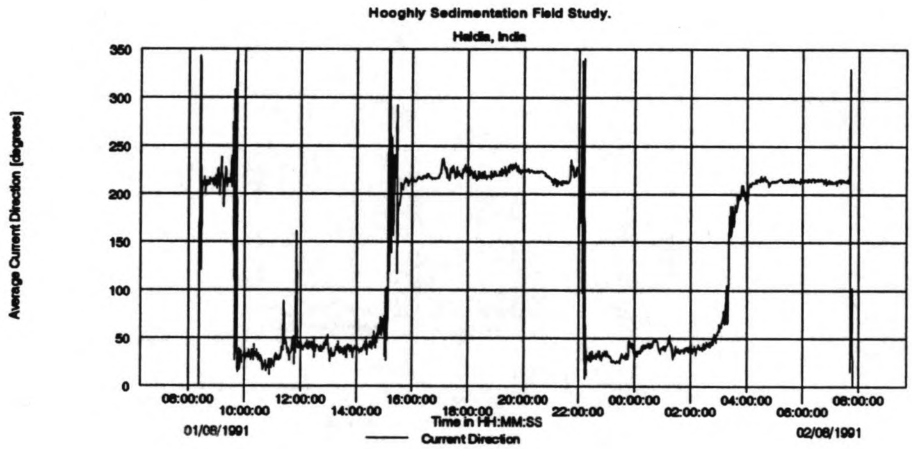

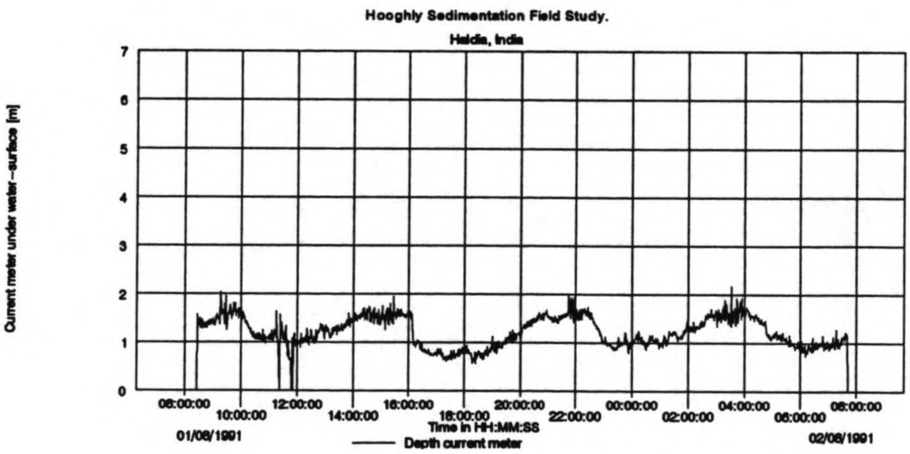

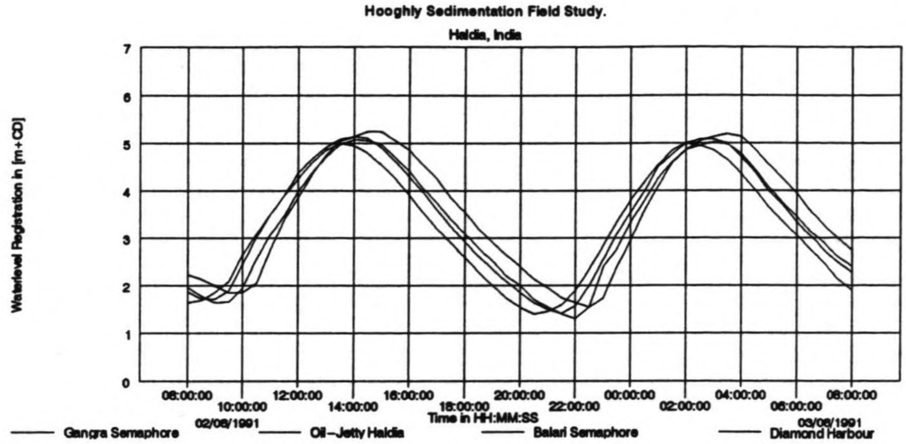

KP8
02/08/91

Figure 2.2.1.4

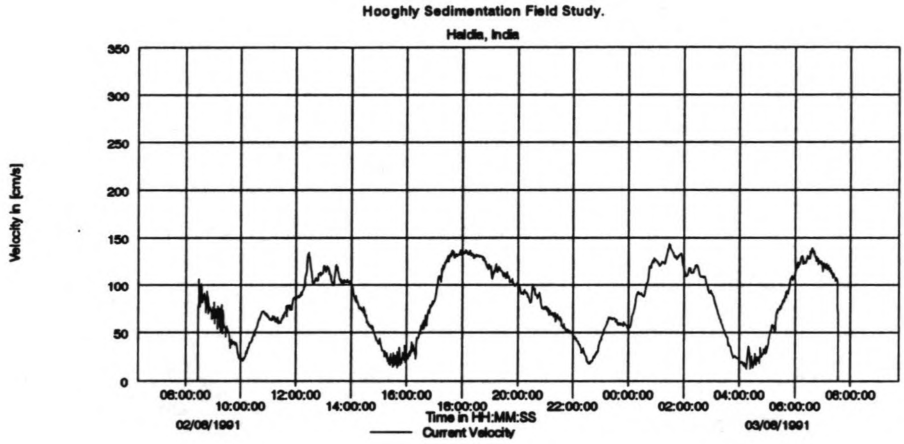

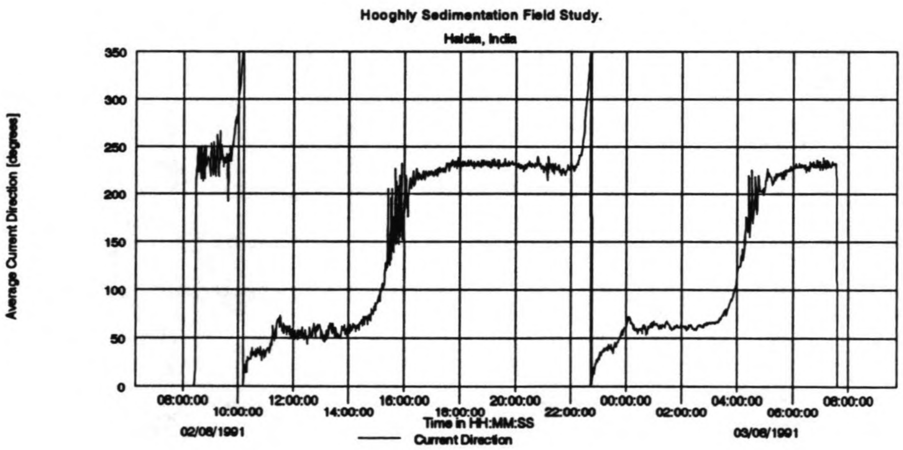

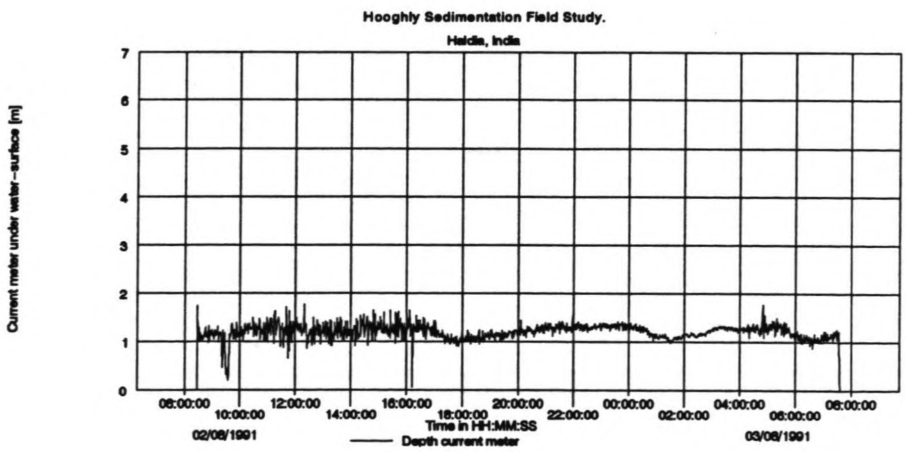

TRW
03/08/91

Figure 2.2.1.5

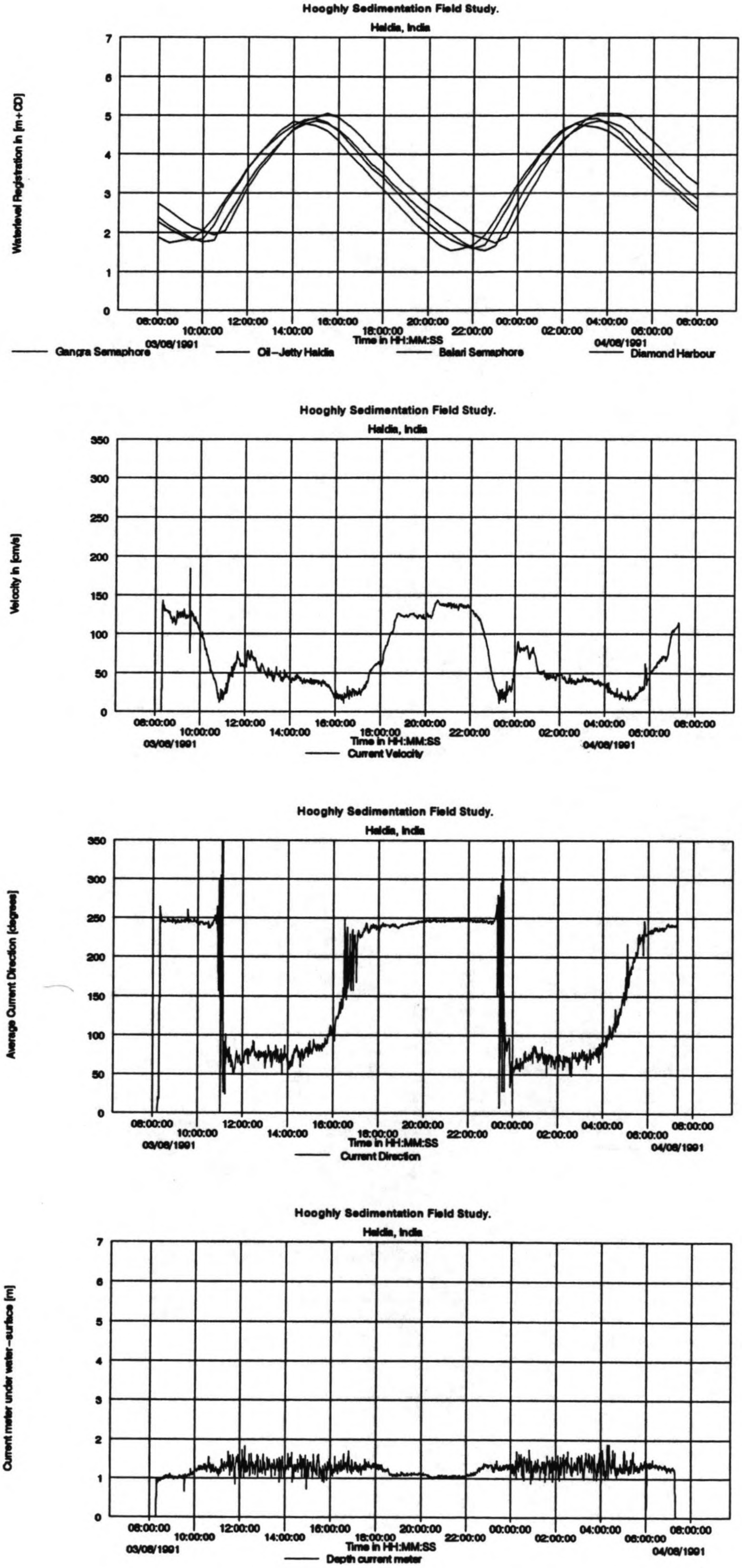

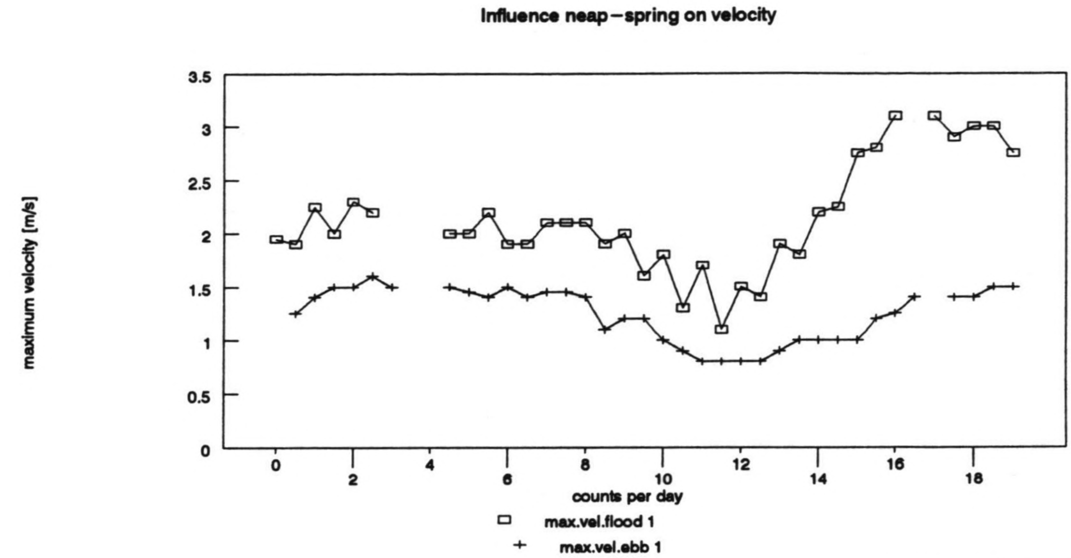

Figure 2.2.2.1

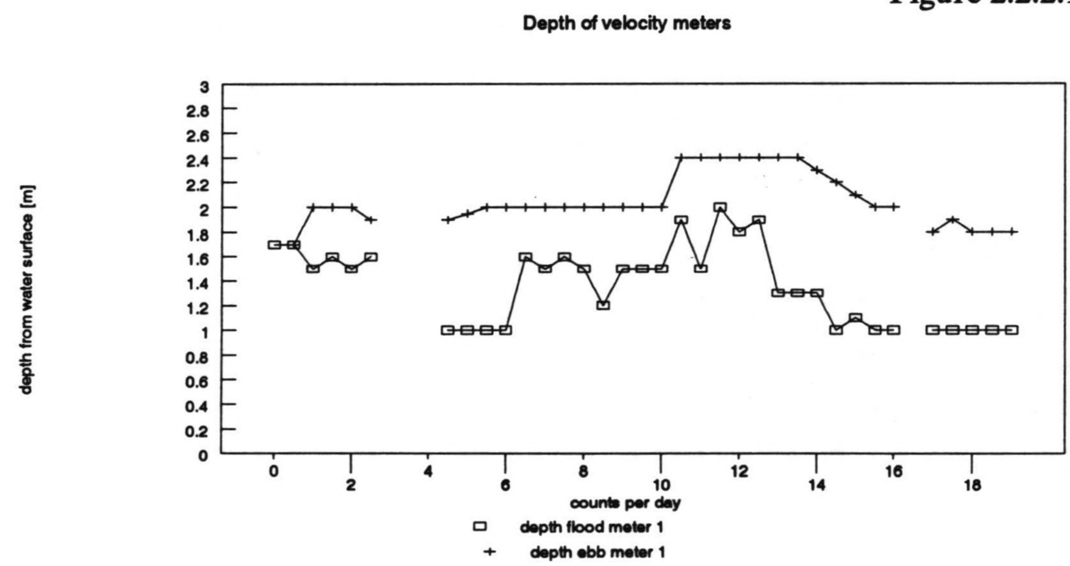

Figure 2.2.2.2

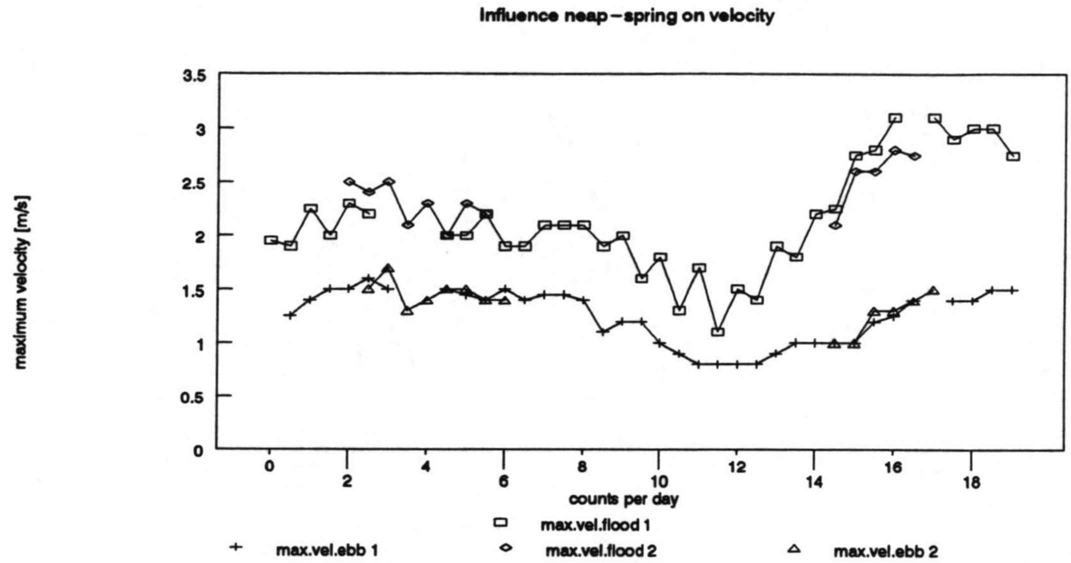

Figure 2.2.2.3

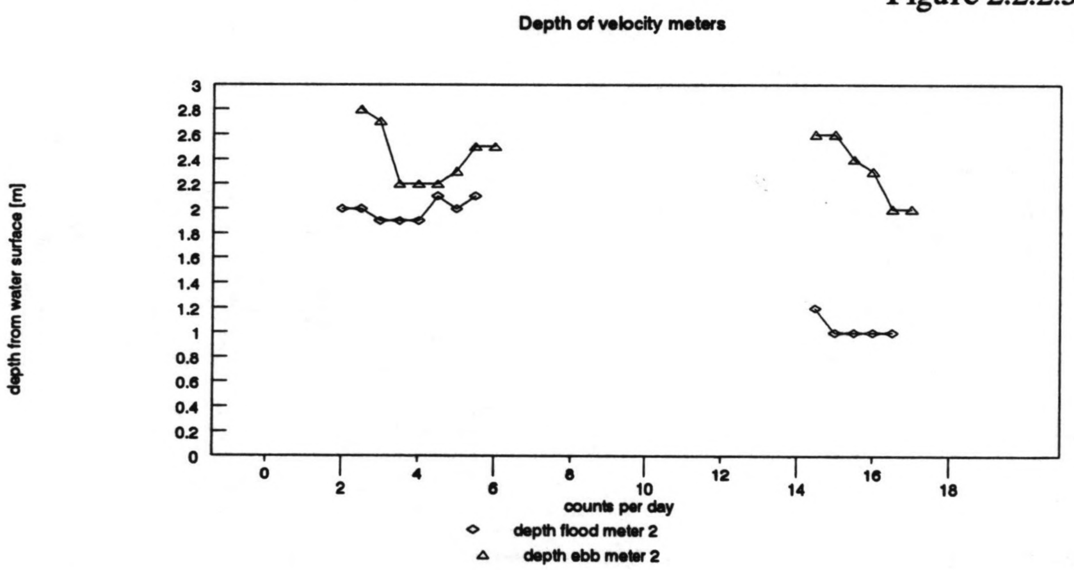

Figure 2.2.2.4

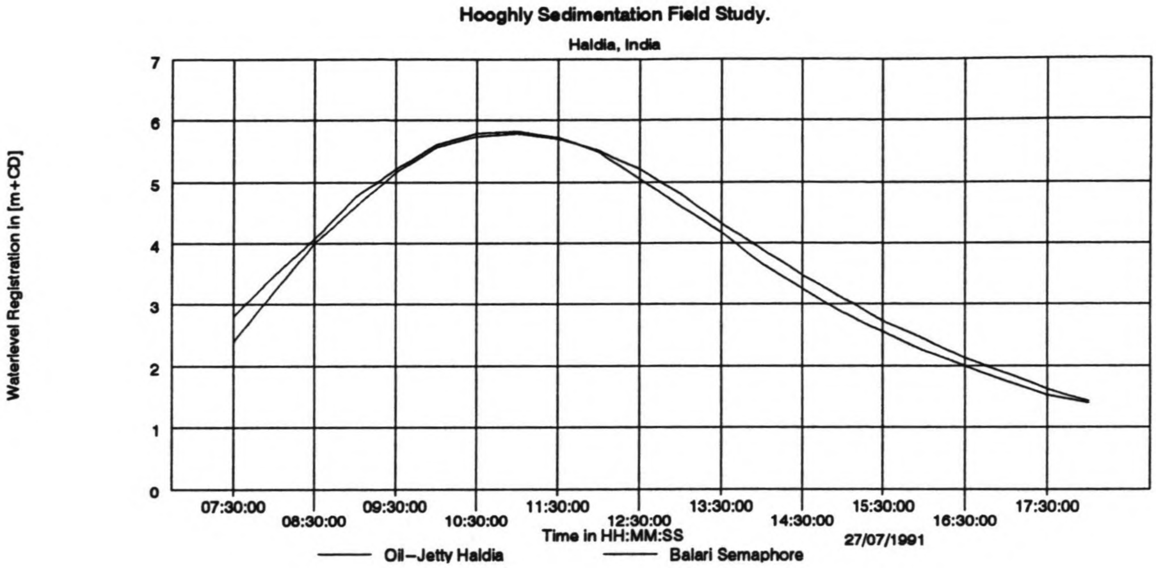

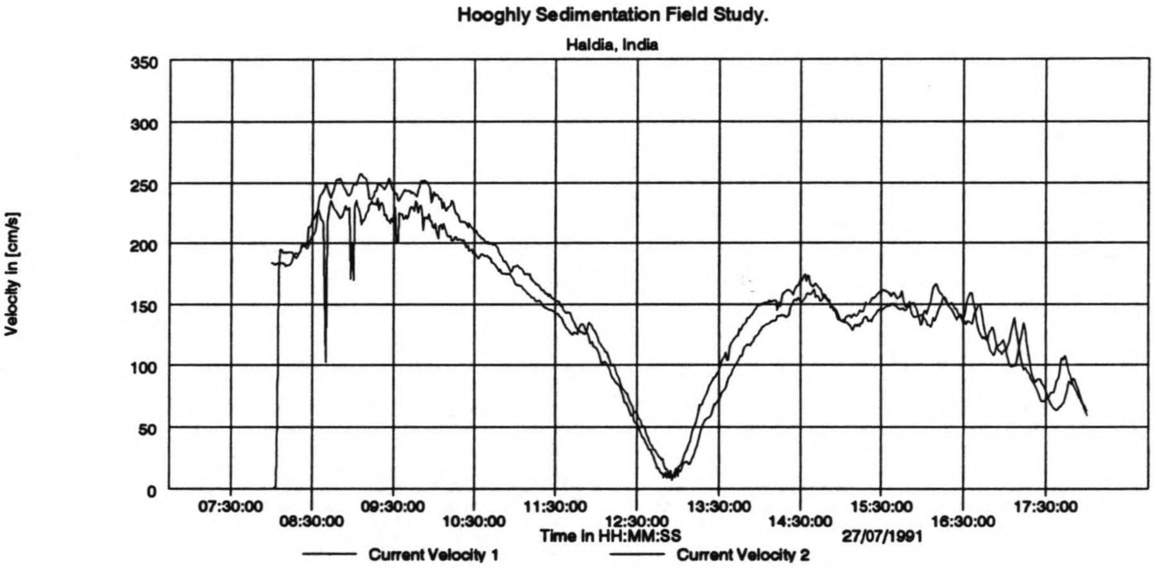

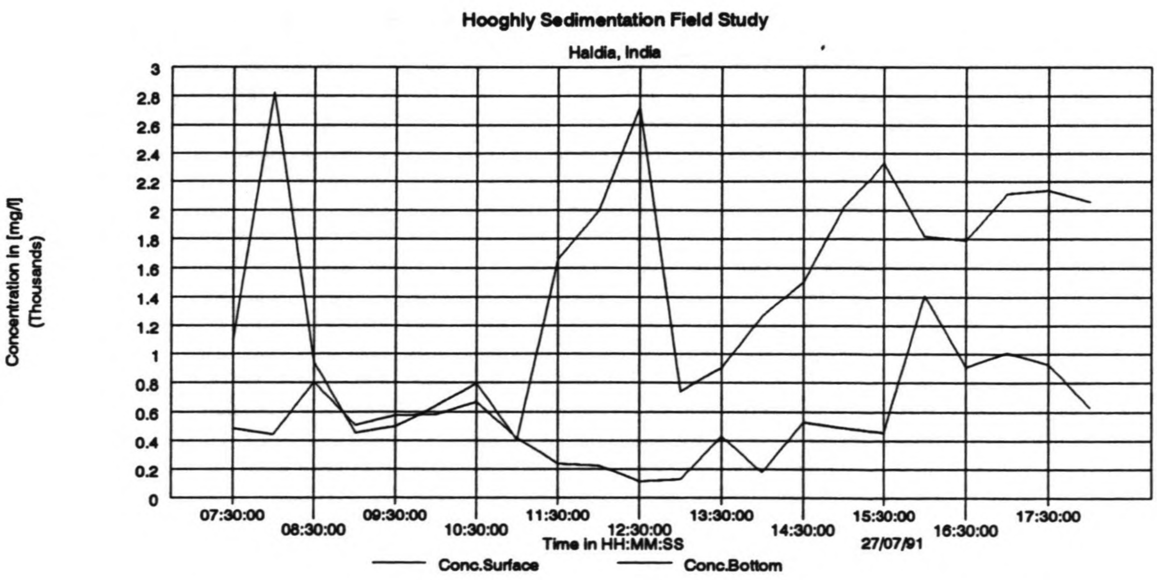

I-A 27/07/91

Figure 2.4.1

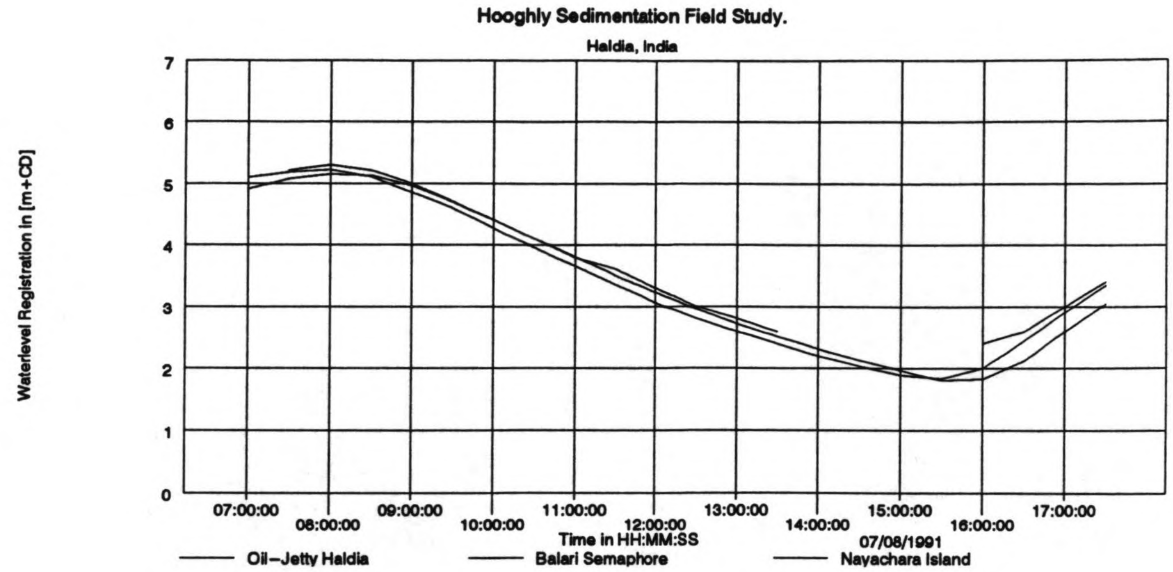

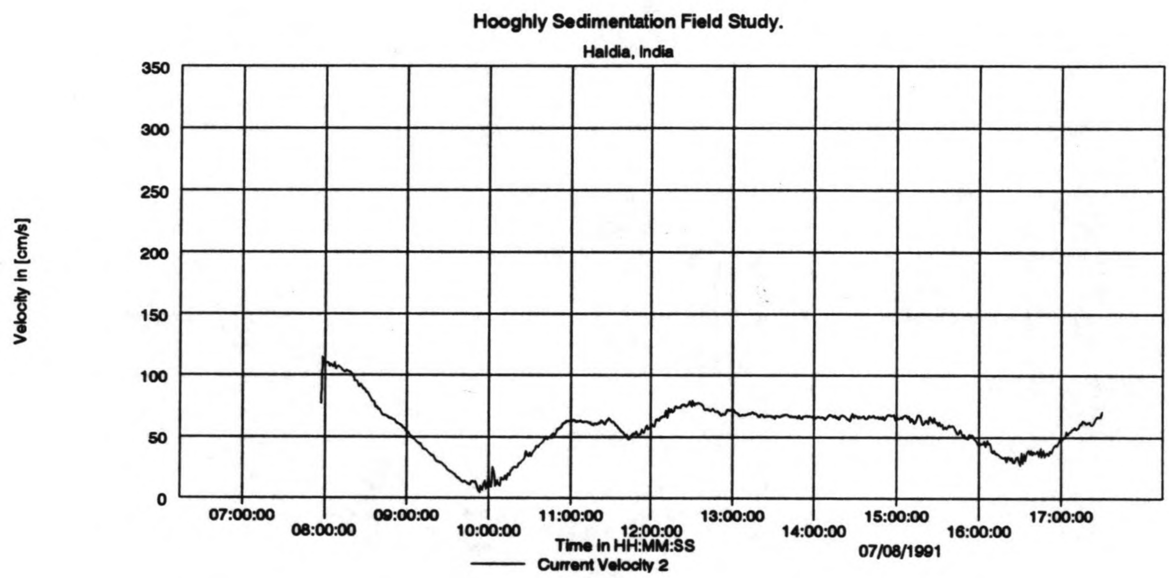

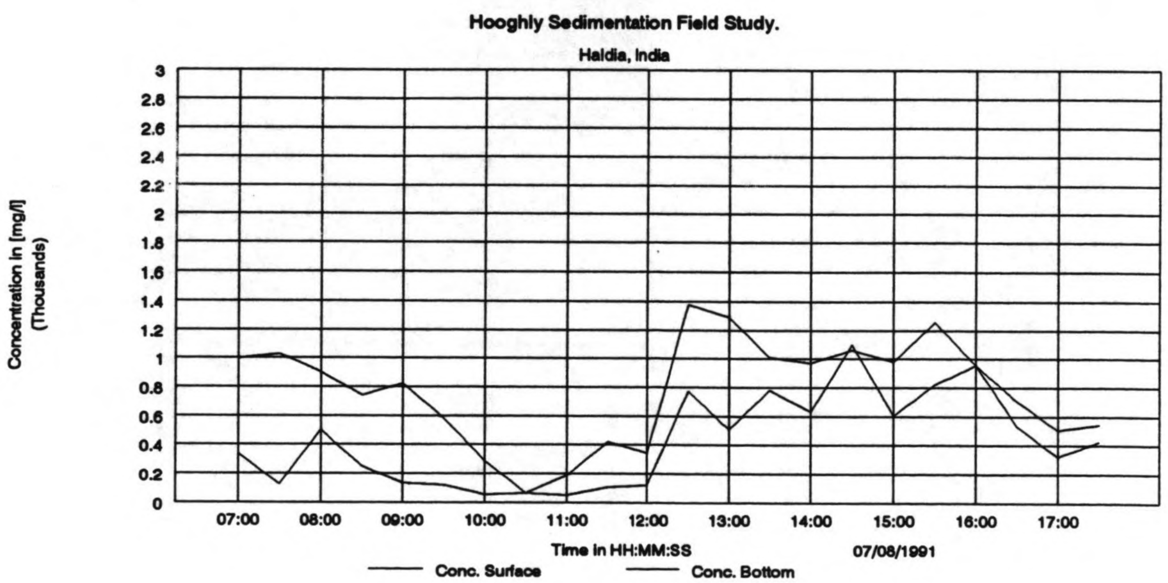

II–A 07/08/91 Figure 2.4.2

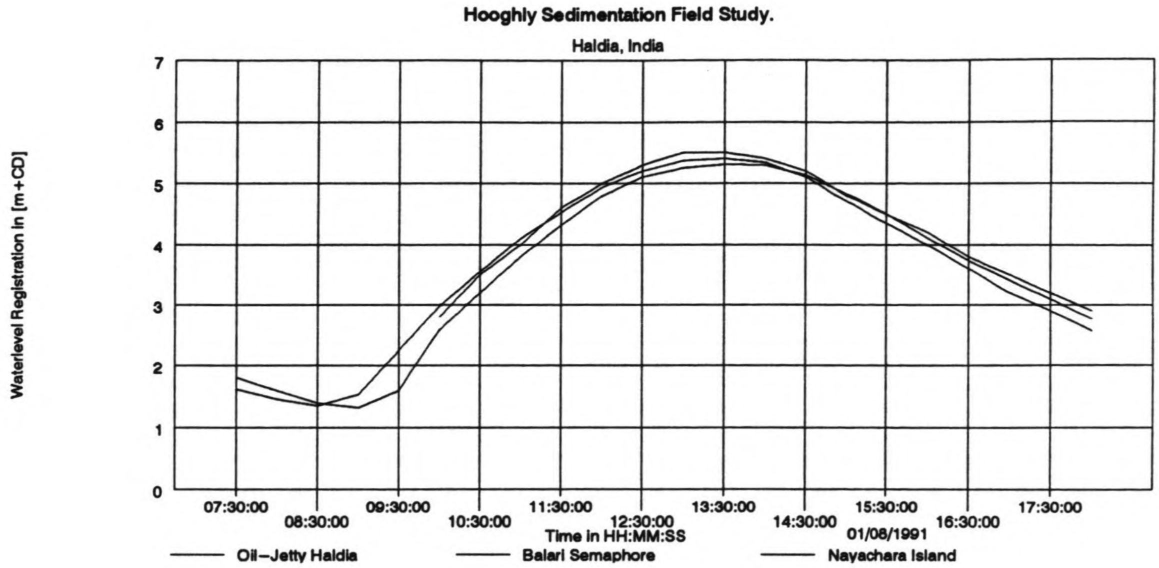

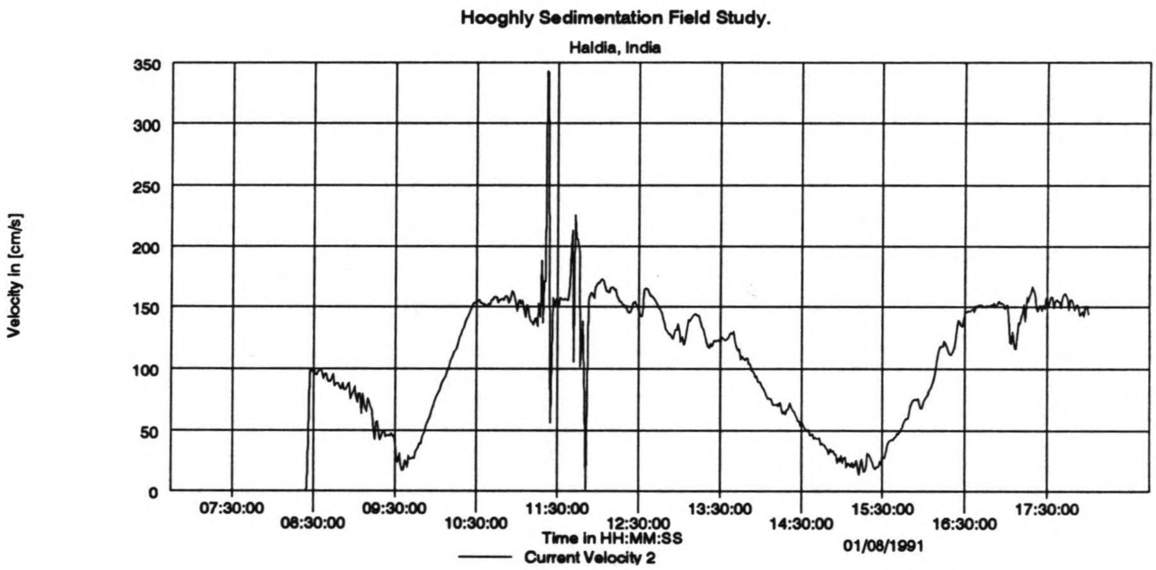

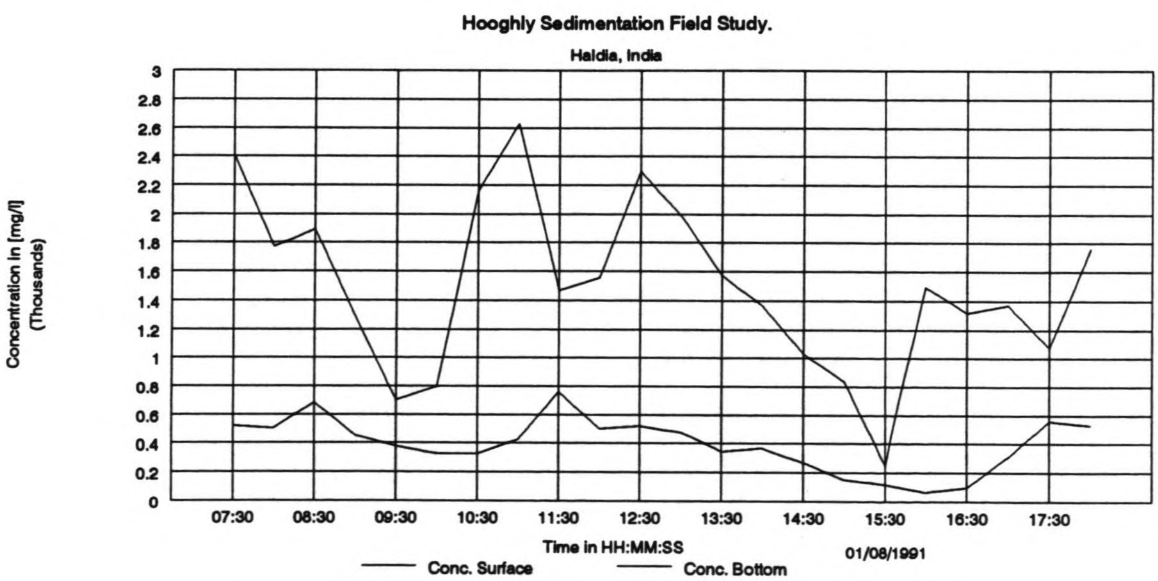

III–B 01/08/91 Figure 2.4.3

Appendix 2.2

Table 2.3

I–A	Velocity flood [m/s]	Velocity ebb [m/s]	Velocity flood [m/s]	Velocity ebb [m/s]	Depth flood [m]	Depth ebb [m]	Depth flood [m]	Depth ebb [m]
Date	Meter 1		Meter 2		Meter 1		Meter 2	
25/07/91	1.95				1.7			
	1.9	1.25			1.7	1.7		
26/07/91	2.25	1.4			1.5	2		
	2	1.5			1.6	2		
27/07/91	2.3	1.5	2.5		1.5	2	2	
	2.2	1.6	2.4	1.5	1.6	1.9	2	2.8
28/07/91		1.5	2.5	1.7			1.9	2.7
			2.1	1.3			1.9	2.2
29/07/91			2.3	1.4			1.9	2.2
	2	1.5	2	1.5	1	1.9	2.1	2.2
30/07/91	2	1.45	2.3	1.5	1	1.95	2	2.3
	2.2	1.4	2.2	1.4	1	2	2.1	2.5
31/07/91	1.9	1.5		1.4	1	2		2.5
	1.9	1.4			1.6	2		
01/08/91	2.1	1.45			1.5	2		
	2.1	1.45			1.6	2		
02/08/91	2.1	1.4			1.5	2		
	1.9	1.1			1.2	2		
03/08/91	2	1.2			1.5	2		
	1.6	1.2			1.5	2		
04/08/91	1.8	1			1.5	2		
	1.3	0.9			1.9	2.4		
05/08/91	1.7	0.8			1.5	2.4		
	1.1	0.8			2	2.4		
06/08/91	1.5	0.8			1.8	2.4		
	1.4	0.8			1.9	2.4		
07/08/91	1.9	0.9			1.3	2.4		
	1.8	1			1.3	2.4		
08/08/91	2.2	1			1.3	2.3		
	2.25	1	2.1	1	1	2.2	1.2	2.6
09/08/91	2.75	1	2.6	1	1.1	2.1	1	2.6
	2.8	1.2	2.6	1.3	1	2	1	2.4
10/08/91	3.1	1.25	2.8	1.3	1	2	1	2.3
		1.4	2.75	1.4			1	2
11/08/91	3.1			1.5	1	1.8		2
	2.9	1.4			1	1.9		
12/08/91	3	1.4			1	1.8		
	3	1.5			1	1.8		
13/08/91	2.75	1.5			1	1.8		

Table 2.4

Location	Date	Velocity flood Meter 2 [m/s]	Velocity ebb Meter 2 [m/s]	Depth v(max) flood [m]	Meter 2 v(max) ebb [m]	Direction flood [dgr]	Direction ebb [dgr]
I–B	25/07/91						
		2	1.5	1.4	2.1	75	250
	26/07/91	2.4	1.5	1.2	2.4		250
I–C	26/07/91						
		2	0.9	1	2.2	75	270
	27/07/91		1.25		1.8		270
	28/07/91						
	29/07/91						
	30/07/91						
III–A	31/07/91	1.8	2	1	1	40	220
III–B	01/08/91	1.6	1.6	1	0.8	35	225
		1.6	1.75	1	1	40	220
KP8	02/08/91						
		1.2	1.4	1.2	1	60	230
	03/08/91	1.4	1.4	1	1	65	230
TW	03/08/91	0.5	1.25	1.2	1	75	250
			1.4		1		250
	04/08/91	0.5		1.2		75	
III–C	04/08/91						
		0.8	1.4	2.2	1.8	40	220
	05/08/91	0.9	1.2	2.2	2	40	220
II–C	05/08/91						
		0.5	0.7	1	0.5	70	225
	06/08/91		0.8	1	0.2	70	
II–B	06/08/91						
		0.8	0.8	1	1	75	250
	07/08/91	1.3	1	0.8	1	75	250
II–A	07/08/91						
		1.5	0.7	0.8	1	70	250
	08/08/91	2	0.75	0.6	1	70	250

Table 2.6

Figure	Measuring date	Location	Max. velocity flood [m/s]	Max. velocity ebb [m/s]	Max. velocity flood [m/s] in I−A	Max. velocity ebb [m/s] in I−A
2.2.1.1	27/07/91	I−A	2.25	1.5		
2.2.1.2	07/08/91	II−A	1.5 − 1.8	0.7 − 1.0	1.8 − 1.9	0.9 − 1
2.2.1.3	01/08/91	III−B	1.7	1.7	2.1	1.45
2.2.1.4	02/08/91	KP8	1.3	1.3	1.9 − 2.1	1.1 − 1.4
2.2.1.5	03/08/91	TRW	0.5	1.3	1.6 − 2	1.2

Figure	Measuring date	Location	Low water at Oil Jetty [m +CD]	High water at Oil Jetty [m +CD]	current direction flood [^{0}]	current direction ebb [^{0}]
2.2.1.1	27/07/91	I−A	1.5	5.5 − 6	70	250
2.2.1.2	07/08/91	II−A	1.7	5.2	70	230 − 275
2.2.1.3	01/08/91	III−B	1.5	5.5	40	225
2.2.1.4	02/08/91	KP8	1.5	5.2	60	240
2.2.1.5	03/08/91	TRW	1.8	5	75	250

Appendix 3.1

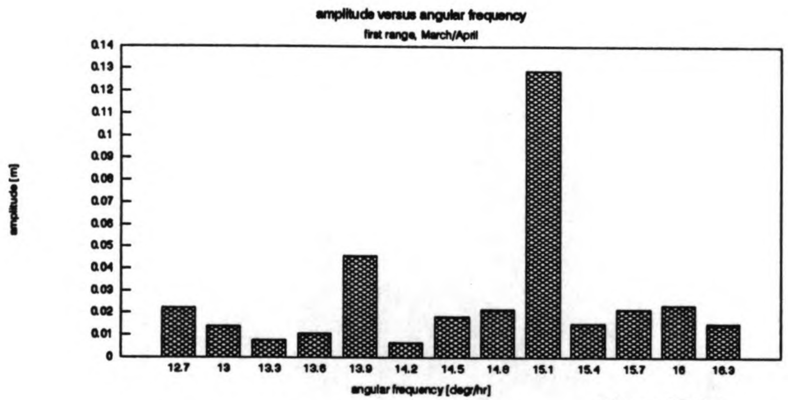

Figure 3.3.2.1

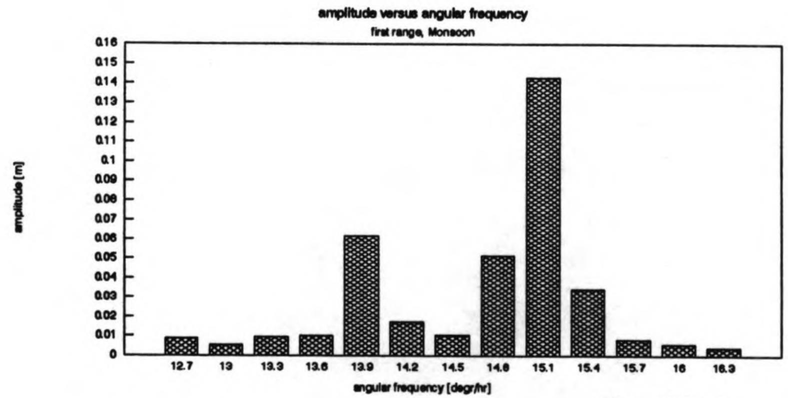

Figure 3.3.2.2

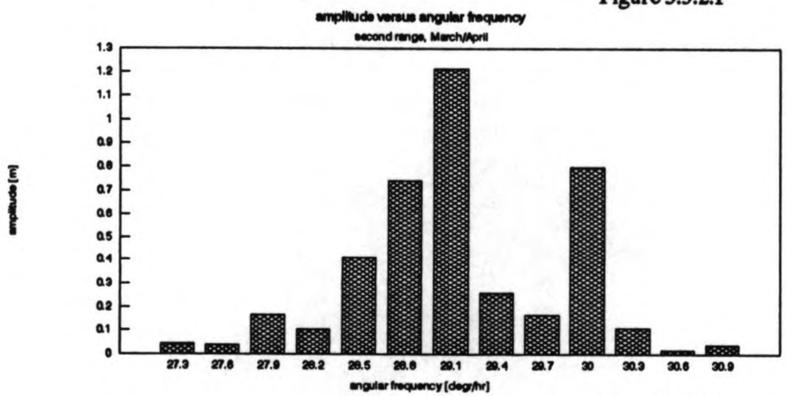

Figure 3.3.2.3

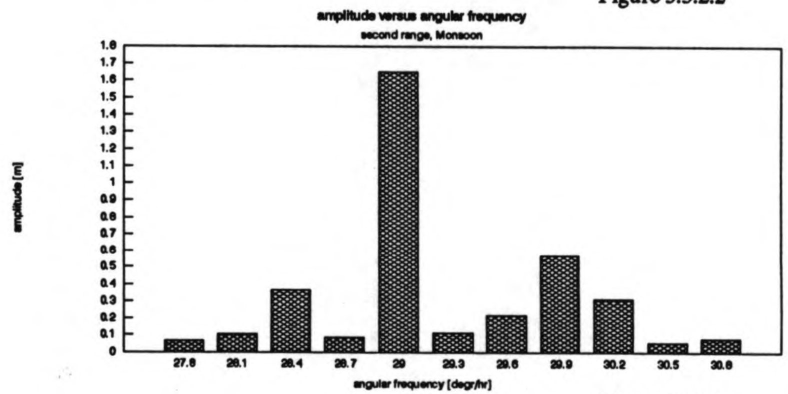

Figure 3.3.2.4

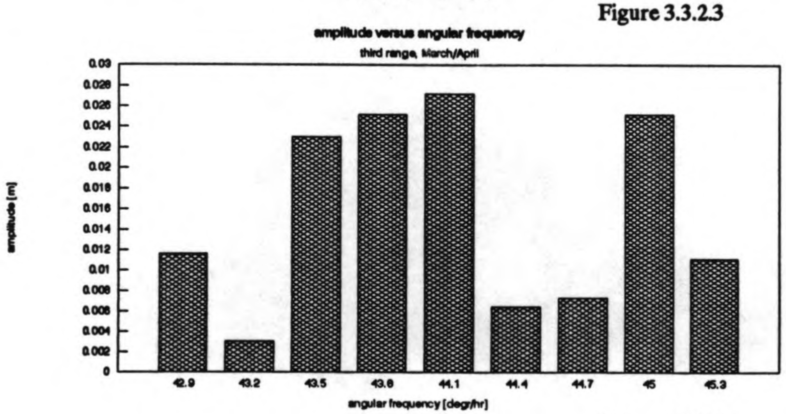

Figure 3.3.2.5

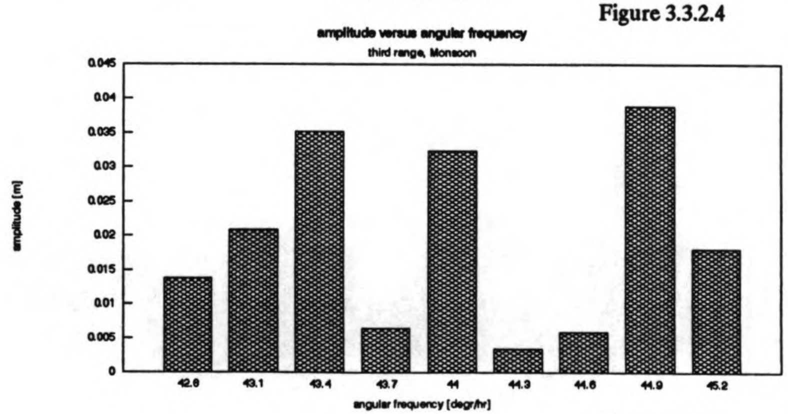

Figure 3.3.2.6

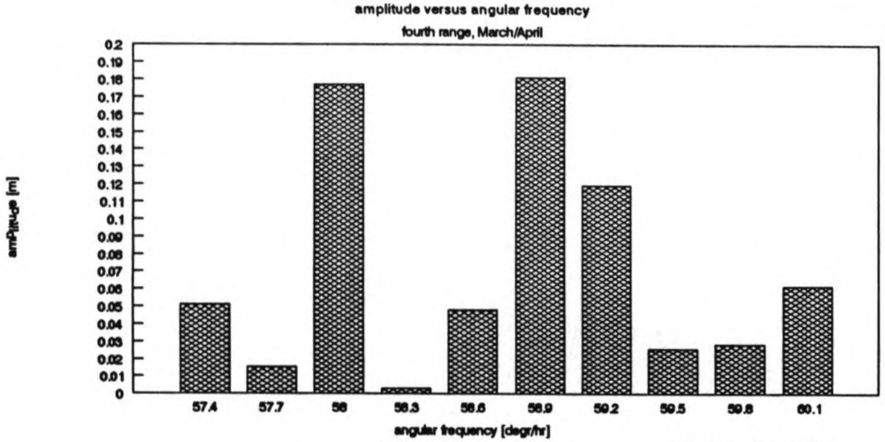

Figure 3.3.2.7

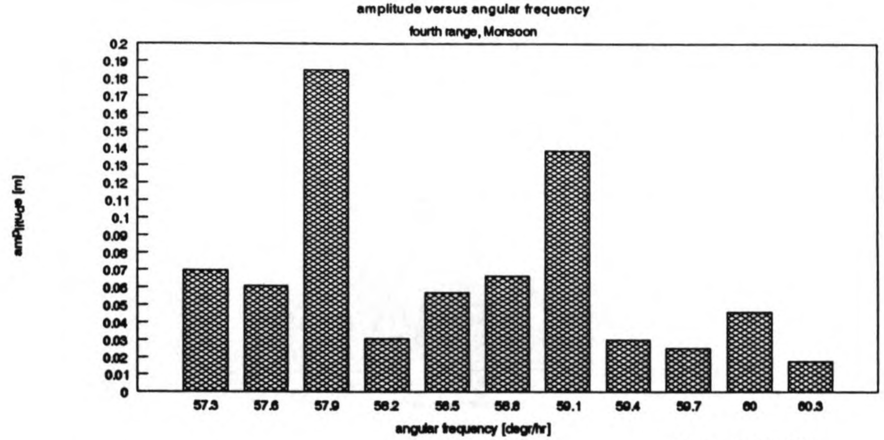

Figure 3.3.2.8

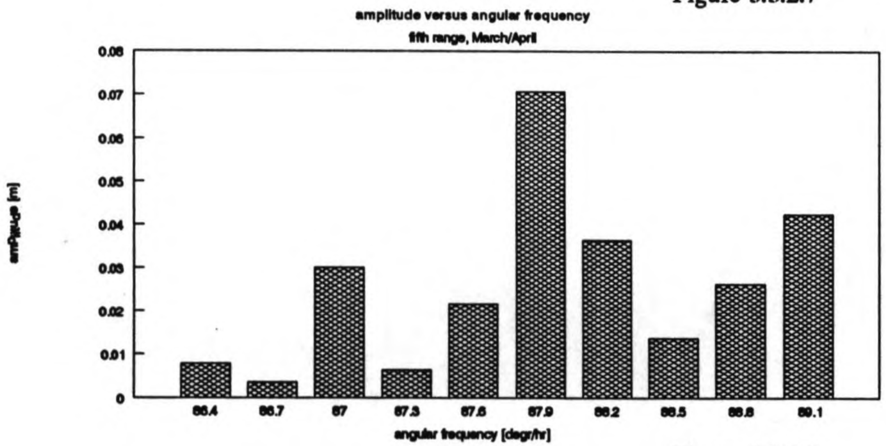

Figure 3.3.2.9

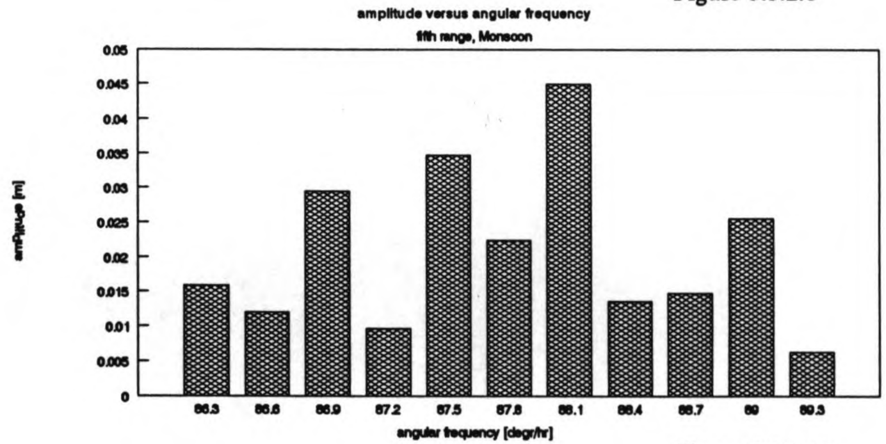

Figure 3.3.2.10

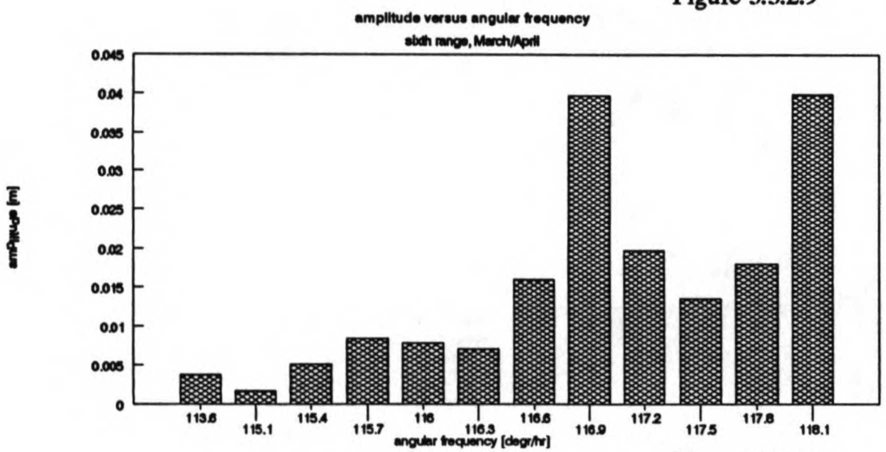

Figure 3.3.2.11

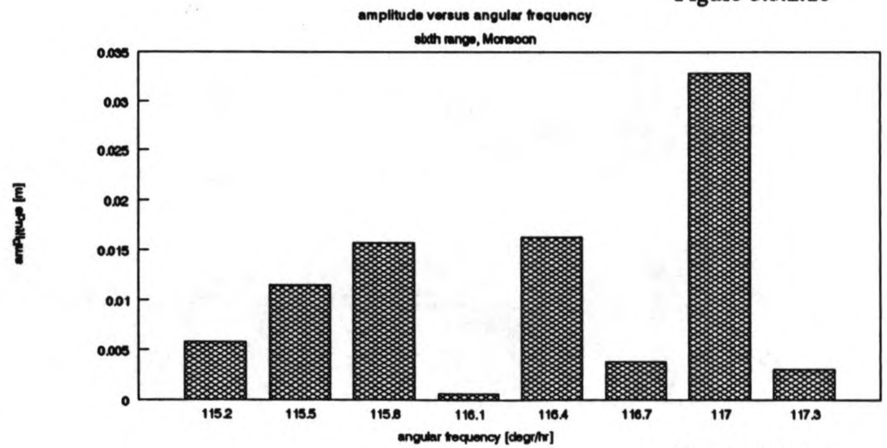

Figure 3.3.2.12

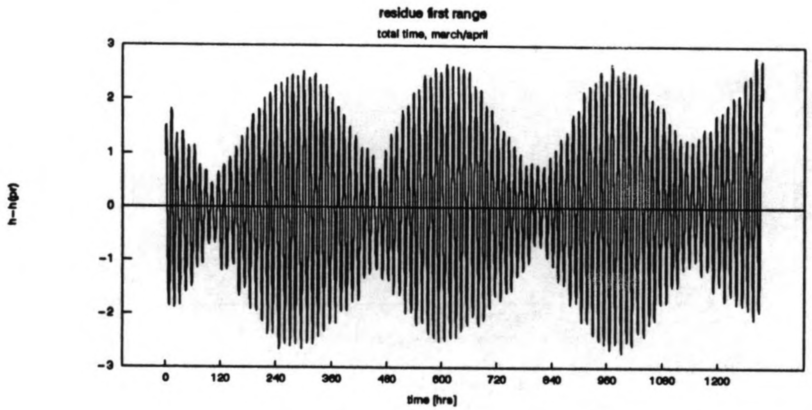

Period:
06/03/91
00:00

28/04/91
23:30

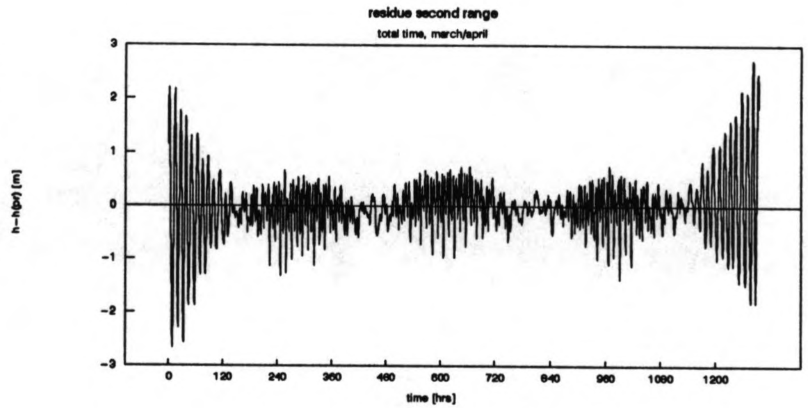

Period:
06/03/91
00:00

09/03/91
00:00

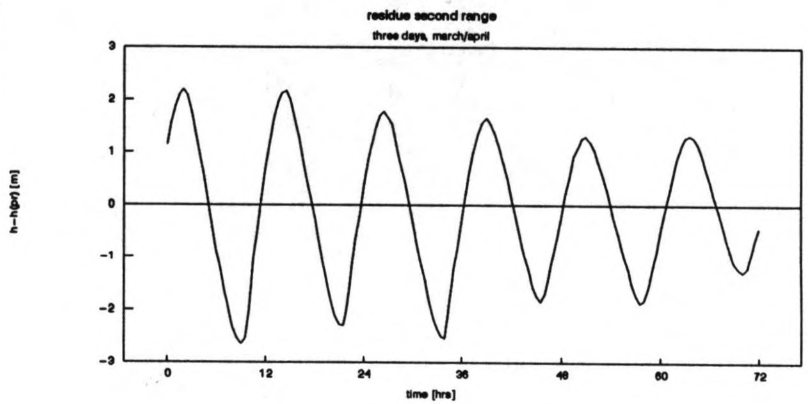

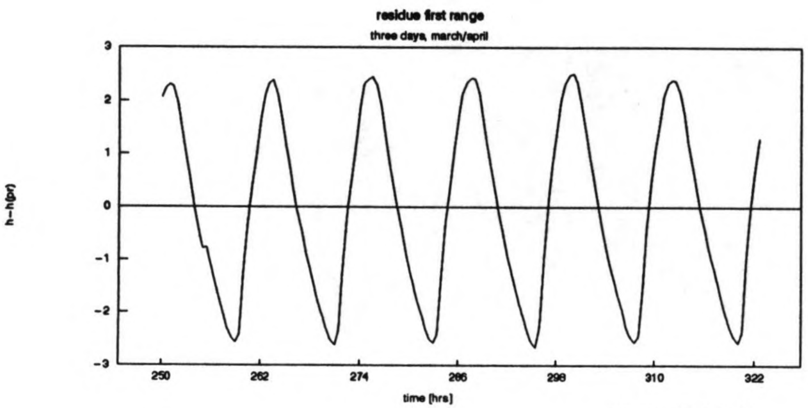

Figure 3.3.2.13

Period:
16/03/91
10:00

19/03/91
10:30

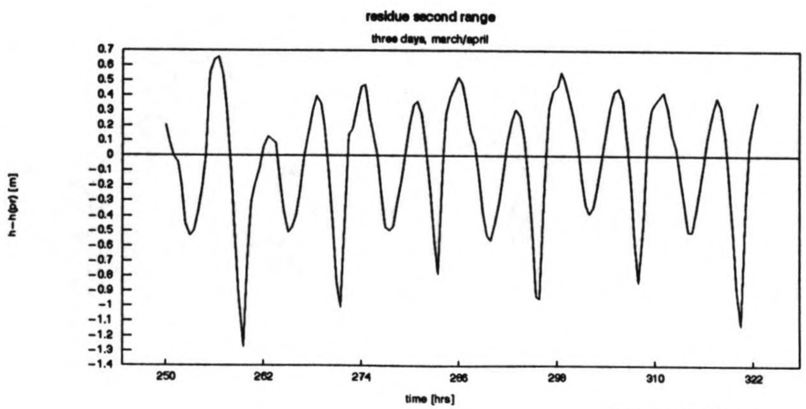

Figure 3.3.2.14

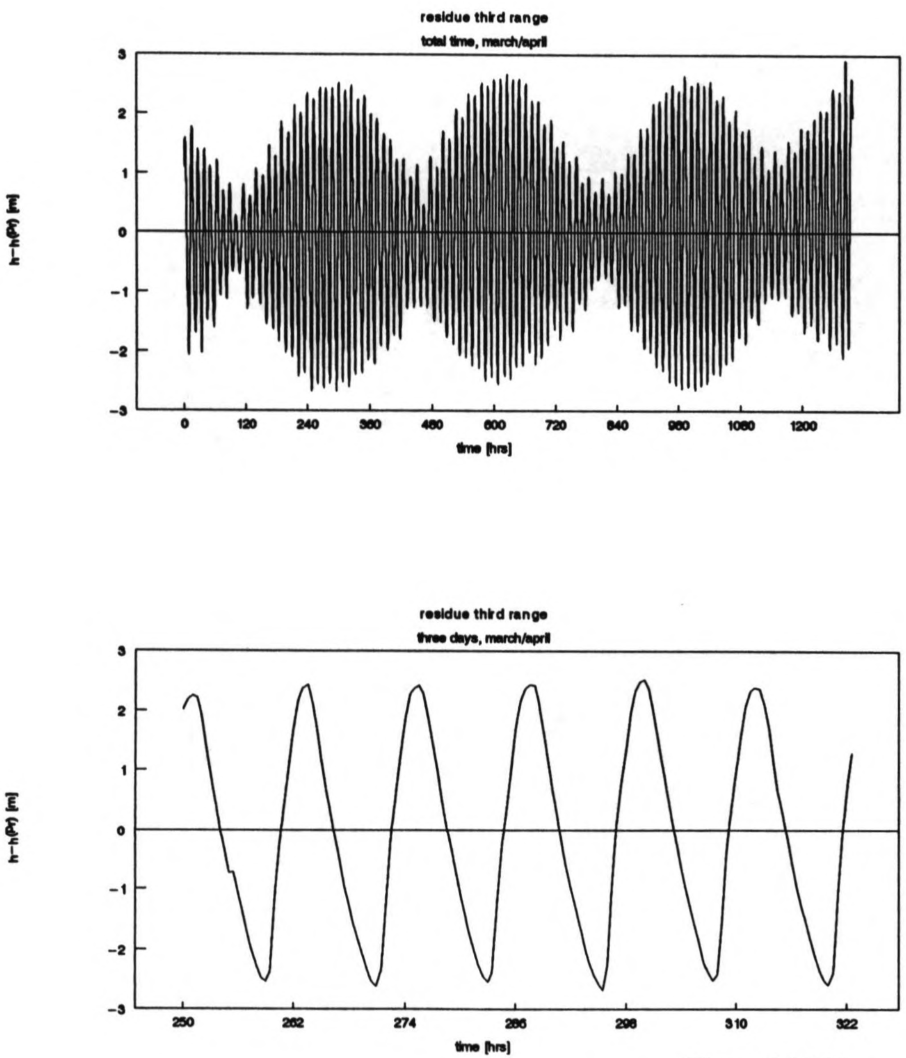

Figure 3.3.2.15

Period:
06/03/91
00:00

28/04/91
23:30

Period:
16/03/91
10:00

19/03/91
10:30

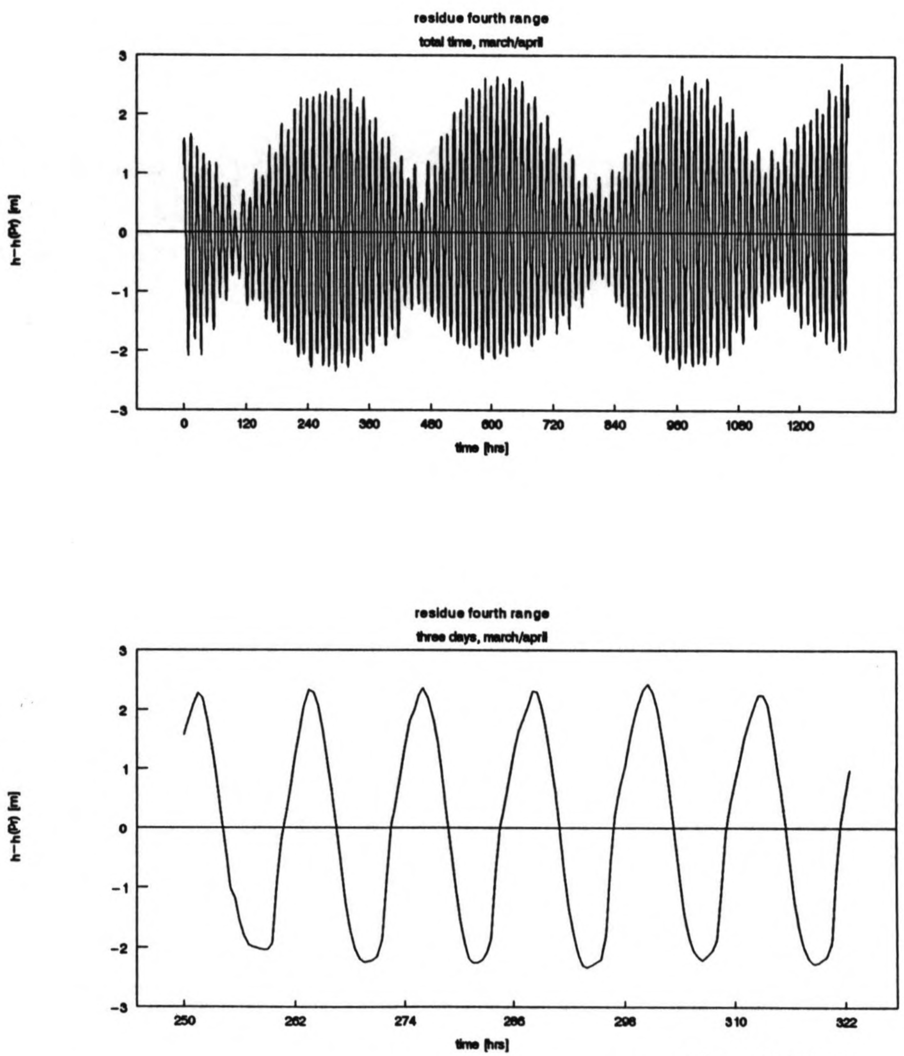

Figure 3.3.2.16

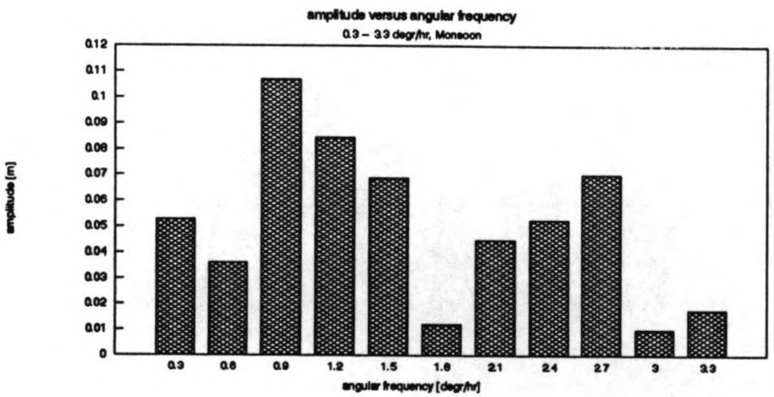

Figure 3.3.2.17

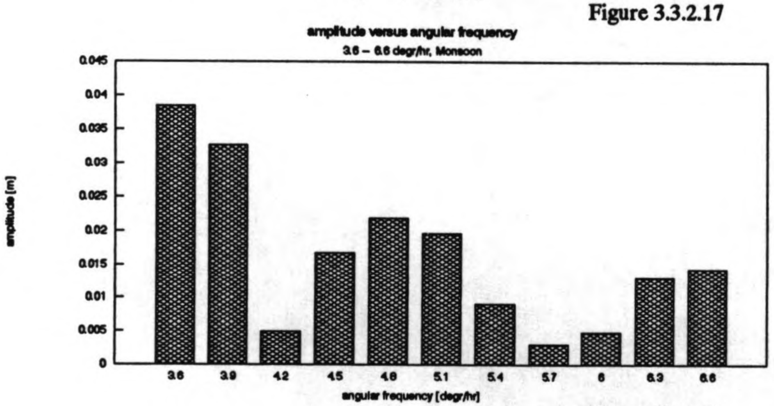

Figure 3.3.2.18

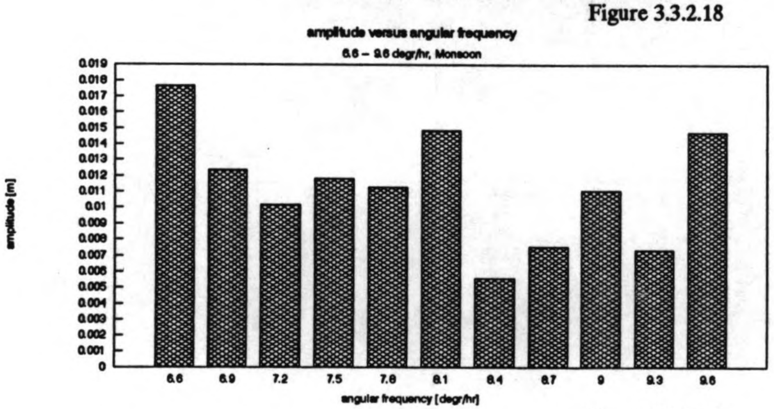

Figure 3.3.2.19

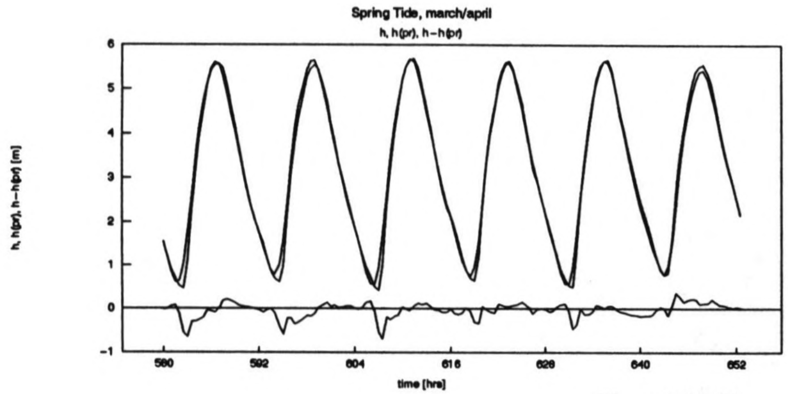

Period:
30/03/91
04:00

02/04/91
04:00

Figure 3.4.1.17

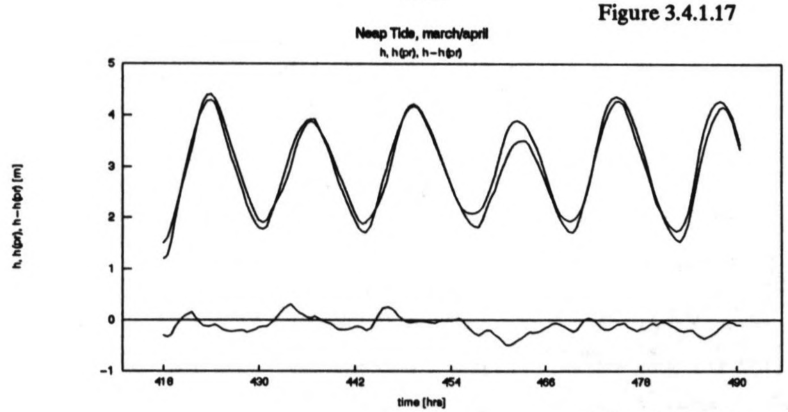

Period:
23/03/91
10:00

26/03/91
10:00

Figure 3.4.1.18

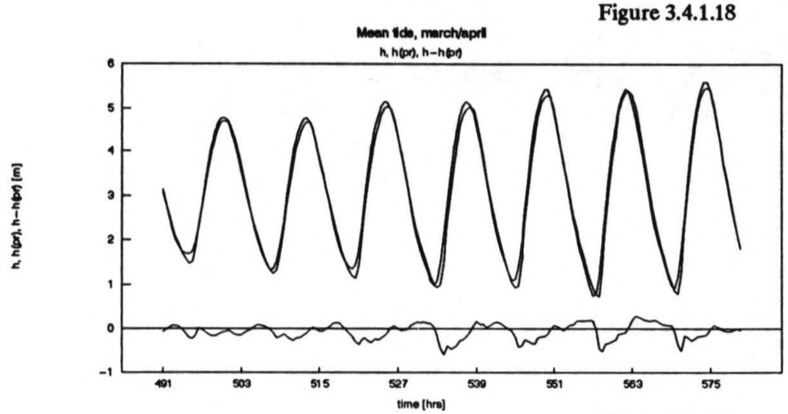

Period:
26/03/91
10:00

29/03/91
23:00

Figure 3.4.1.19

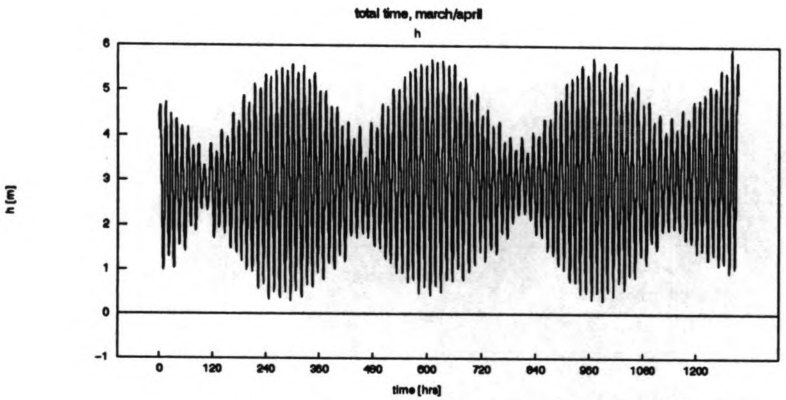

Period:
06/03/91
00:00

28/04/91
23:30

Figure 3.4.3.1

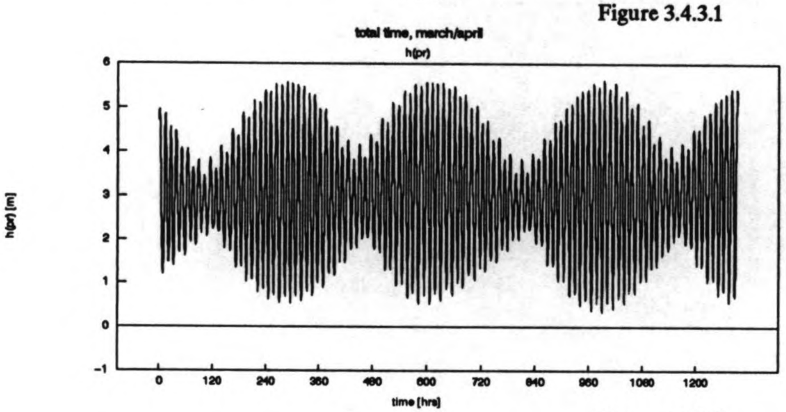

Period:
06/03/91
00:00

28/04/91
23:30

Figure 3.4.3.2

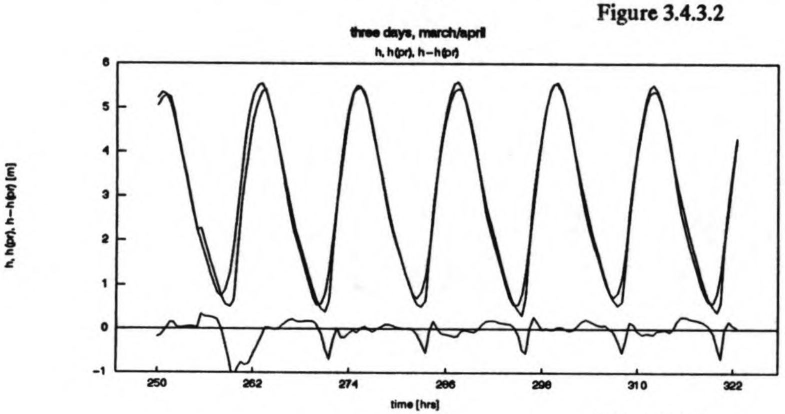

Period:
16/03/91
10:00

19/03/91
10:30

Figure 3.4.3.3

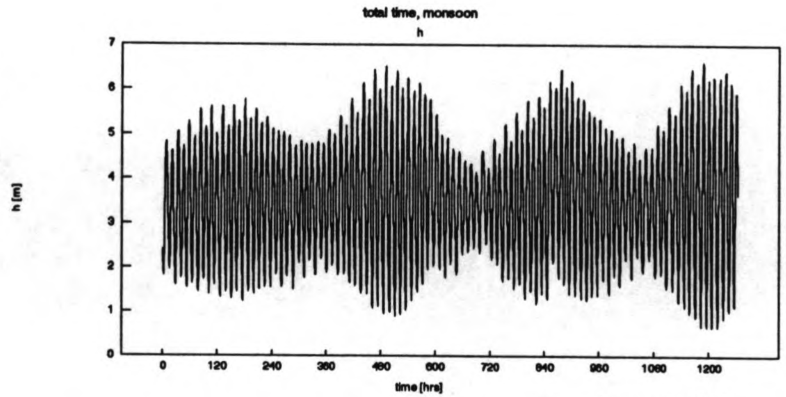

Period:
23/06/91
00:00

14/08/91
00:00

Figure 3.4.3.4

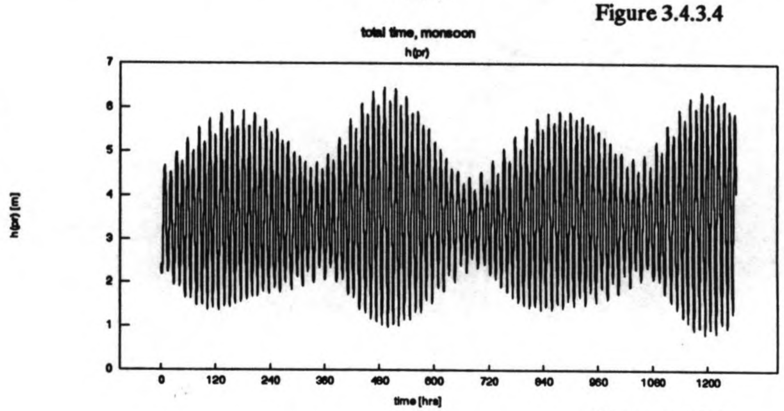

Period:
23/06/91
00:00

14/08/91
00:00

Figure 3.4.3.5

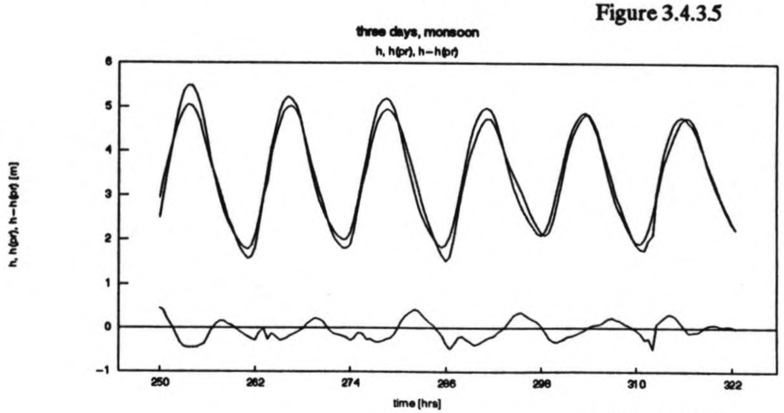

Period:
23/06/91
00:00

26/06/91
00:00

Figure 3.4.3.6

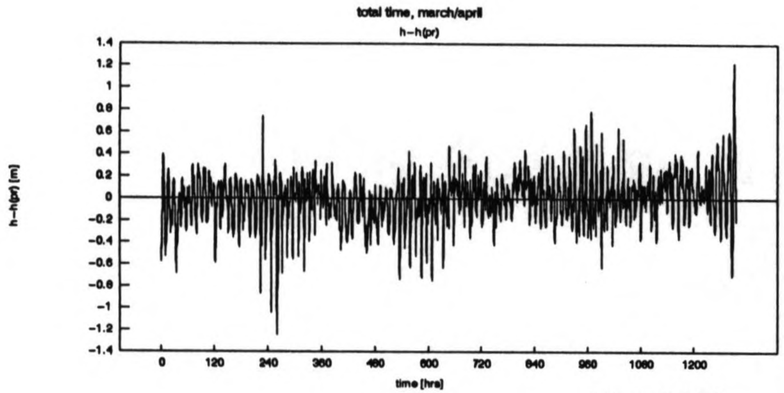

Figure 3.4.3.7

Period:
06/03/91
00:00

28/04/91
23:30

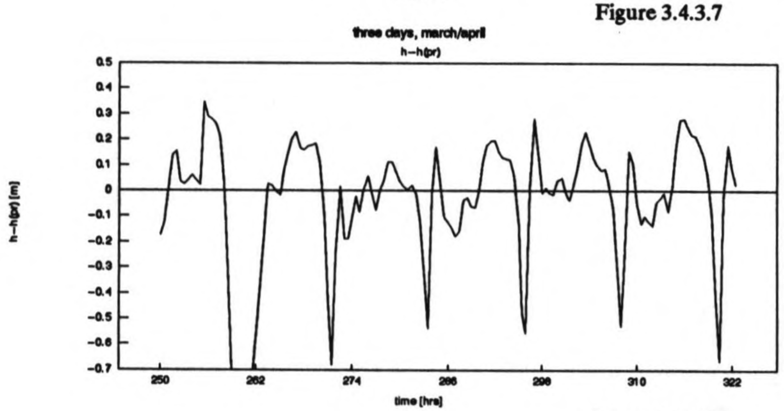

Figure 3.4.3.8

Period:
16/03/91
10:00

19/03/91
10:30

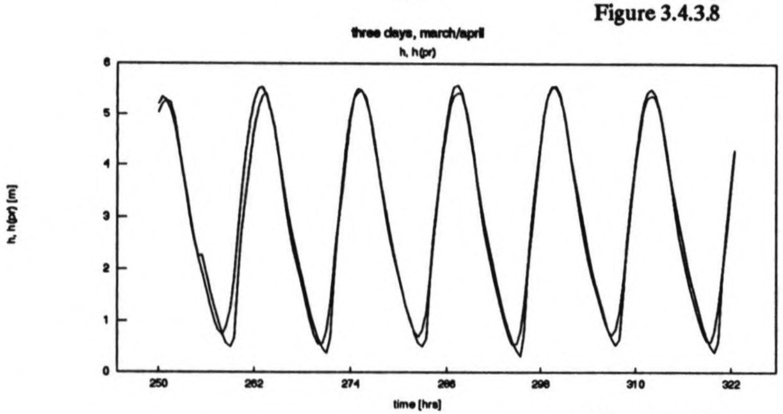

Figure 3.4.3.9

Period:
16/03/91
10:00

19/03/91
10:30

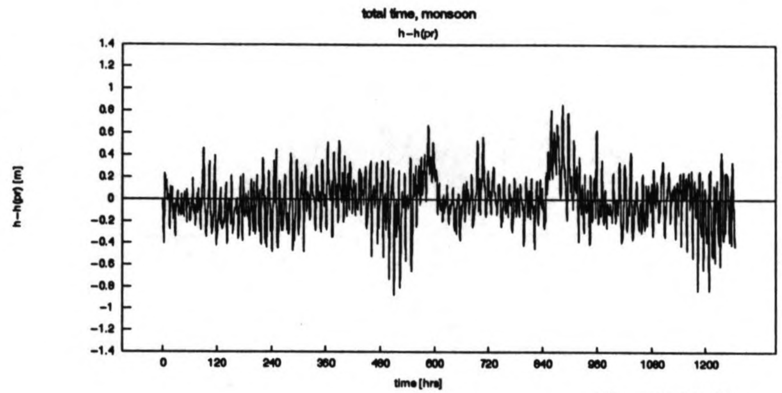

Figure 3.4.3.10

Period:
23/06/91
00:00

14/08/91
16:00

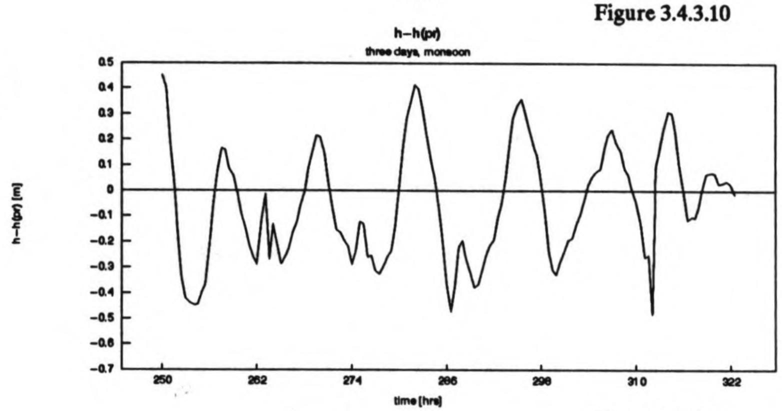

Figure 3.4.3.11

Period:
03/07/91
10:00

06/07/91
10:30

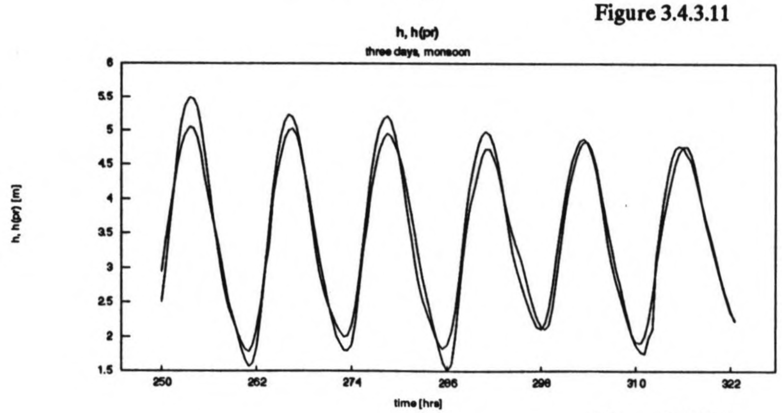

Figure 3.4.3.12

Period:
03/07/91
10:00

06/07/91
10:30

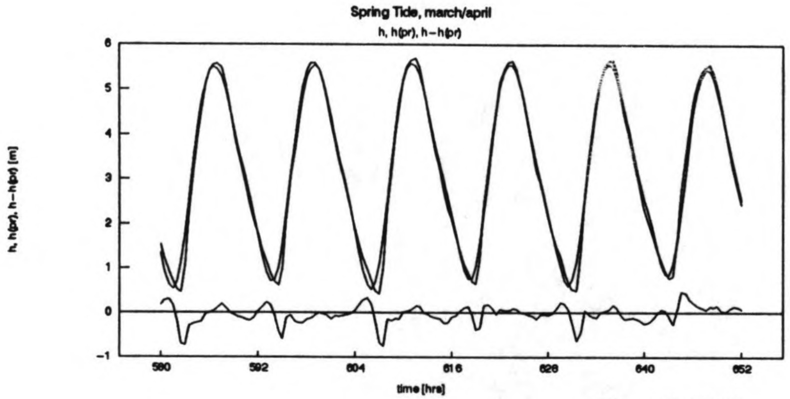

Period:
30/03/91
04:00

02/04/91
04:00

Figure 3.4.3.13

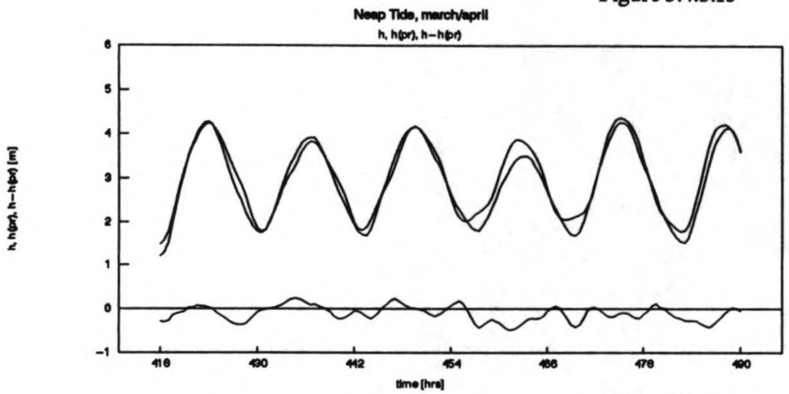

Period:
23/03/91
10:00

26/03/91
10:00

Figure 3.4.3.14

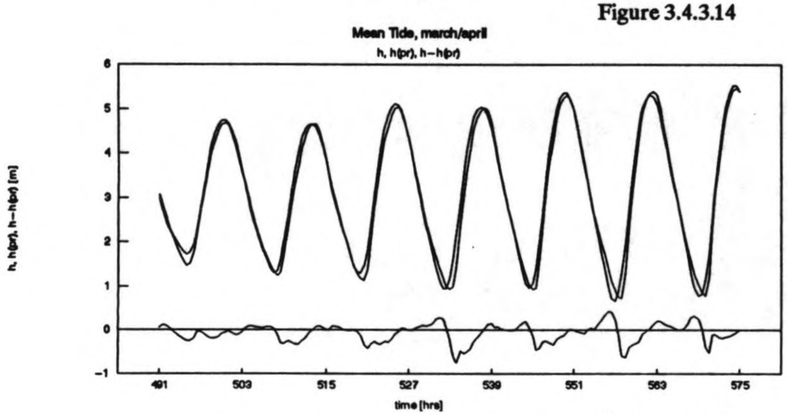

Period:
26/03/91
11:00

29/03/91
23:00

Figure 3.4.3.15

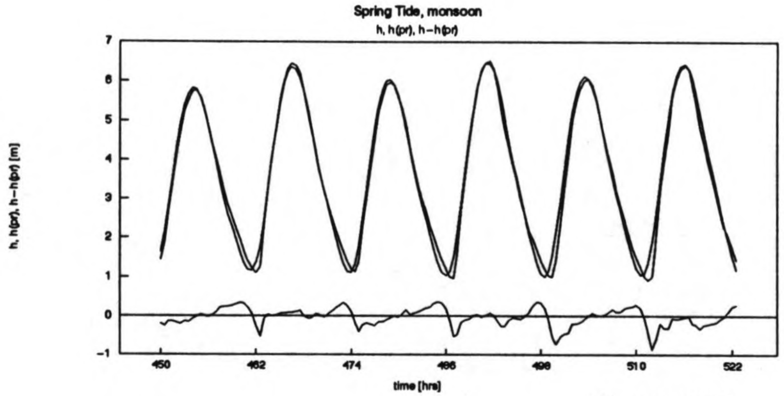

Period:
11/07/91
18:00

14/07/91
18:00

Figure 3.4.3.16

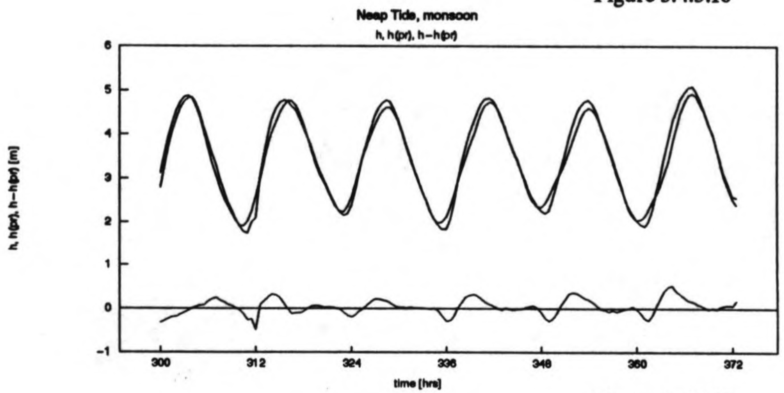

Period:
05/07/91
12:00

08/07/91
12:00

Figure 3.4.3.17

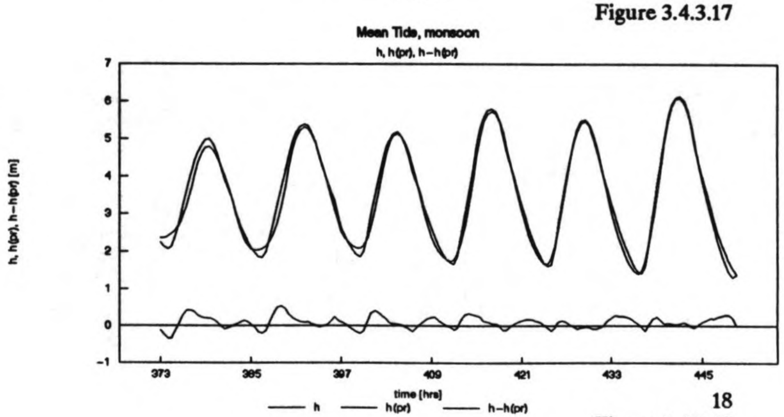

Figure 3.4.3.18

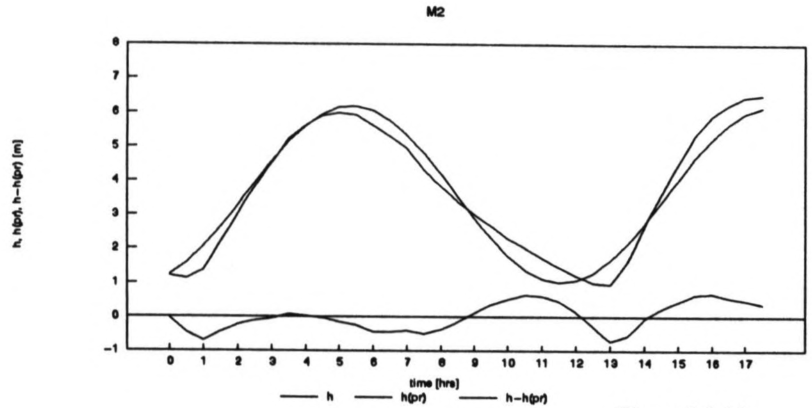

Figure 3.4.4.1

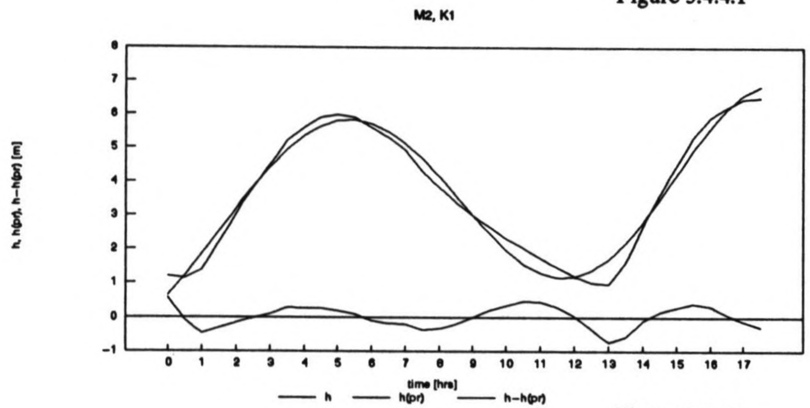

Figure 3.4.4.2

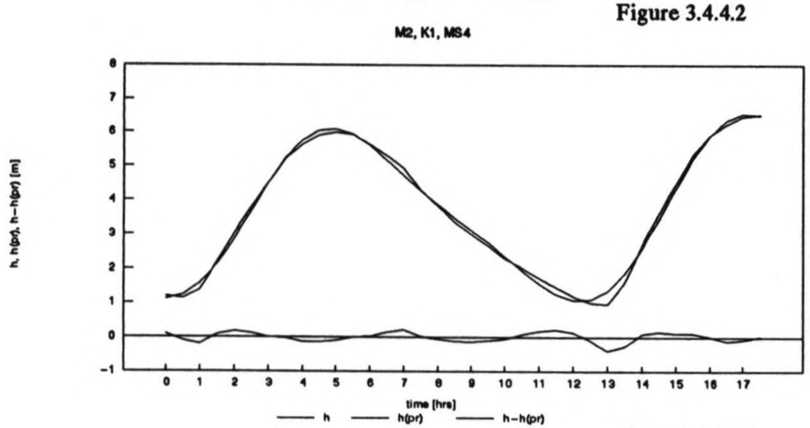

Figure 3.4.4.3

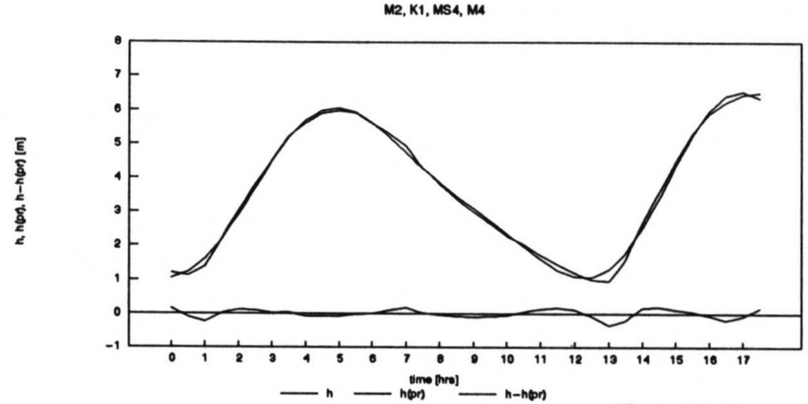

Figure 3.4.4.4

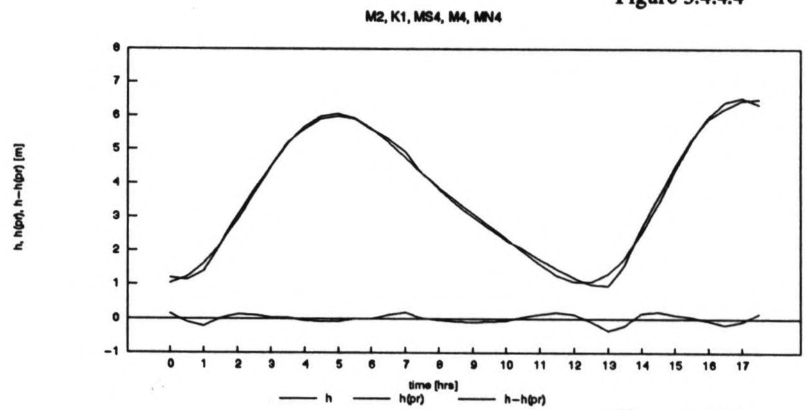

Figure 3.4.4.5

Appendix 3.2

Table 3.1

Name harmonic	Ang.freq. [dgr/hr]	Name shallow	Ang.freq. [dgr/hr]
Sa	0.04	NO1	14.50
Ssa	0.08	SO1	16.06
MSf	1.02	OQ2	27.35
Mm	0.54	2MS2	27.97
Mf	1.10	OP2	28.94
2Q1	12.85	MKS2	29.07
sigma 1	12.93	2MN2	29.53
Q1	13.40	MSN2	30.54
rho 1	13.47	2SM2	31.02
O1	13.94	MO3	42.93
tau 1	14.03	SO3	43.94
M1	14.49	MK3	44.03
NO1	14.50	SK3	45.04
X1	14.57	MN4	57.42
pi 1	14.92	M4	57.97
P1	14.96	SN4	58.44
S1	15.00	MS4	58.98
K1	15.04	MK4	59.07
PSI 1	15.08	S4	60.00
phi 1	15.12	SK4	60.08
theta 1	15.51	2MN6	86.41
J1	15.59	M6	86.95
OO1	16.14	MSN6	87.42
epsilon 1	27.42	2MS6	87.97
2N2	27.90	2MK6	88.05
2MS2	27.97	2SM6	88.98
N2	28.44	MSK6	89.07
nu 2	28.51	3MN8	115.39
M2	28.98	M8	115.94
lamda 2	29.46	2MSN8	116.41
L2	29.53	3MS8	116.95
T2	29.96	2(MS)8	117.97
S2	30.00	2MSK8	113.66
R2	30.04		
K2	30.08		
dzeta 2	30.55		
eta 2	30.63		
M3	43.48		

Table 3.2

	ω [dgs/hr]	σ [hrs^{-1}]
MS_f	1.015894	0.002822
O_1	13.943037	0.038731
P_1	14.958931	0.041655
K_1	15.041069	0.041781
M_2	28.984106	0.080511
S_2	30.000000	0.083333
L_2	29.52848	0.082024
M_4	57.968212	0.161023

Table 3.3

	MS_f	O_1	P_1	K_1	M_2	S_2	L_2	M_4
MS_f	***	1.160	1.073	1.070	0.536	0.518	0.526	0.263
O_1		***	14.25	13.62	0.997	0.934	0.962	0.341
P_1			***	331.6	1.073	1.0	1.032	0.341
K_1				***	1.076	1.003	1.035	0.349
M_2					***	14.77	27.55	0.518
S_2						***	31.81	0.536
L_2							***	0.527
M_4								***

Minimum observation time (in days) to divide the combination of frequencies.

Table 3.4

rank of range	March/April angular frequency [dgr/hr]	Monsoon angular frequency [dgr/hr]	selected harmonic component	preferred above:
first	13.9	13.9	O1	
	15.1	15.1	K1	
second	27.9		2MS2	2N2
	28.2			
	28.5	28.4	N2	
	28.8			
	29.1	29.0	M2	
	29.4	29.6	L2	T2
	29.7			
	30.0	29.9	S2	
	30.3	30.2		
fourth	57.4	57.3	MN4	
		57.6		
	58.0	57.9	M4	
		58.5		
	58.9	58.8	MS4	MK4
	59.2	59.1		
	60.1			
fifth	87.9		2MS6	
below first range	0.3	0.5	Mm	
	0.9		MSf	
	1.5			
	2.7			

Table 3.5 Amplitudes in [m]

ang.freq. [dgr/hr]		amplitude March/April	amplitude Monsoon
MSf	1.015894	0.095	0.124
Mm	0.544375	0.101	0.052
O1	13.94	0.048	0.067
K1	15.04	0.136	0.162
2MS2	27.97	0.108	0.090
N2	28.44	0.188	0.349
M2	28.98	1.585	1.646
L2	29.53	0.052	0.088
S2	30	0.867	0.681
MSN2	30.54	0.023	0.042
2SM2	31.02	0.038	0.008
MN4	57.42	0.041	0.087
M4	57.97	0.185	0.187
MS4	59	0.229	0.174
S4	60	0.066	0.041
2MS6	88	0.087	0.060
2SM6	89	0.046	0.023
3MS8	116.95	0.046	0.037
2(MS)8	117.97	0.042	0.024
J1	15.6	0.013	0.005
MK3	44	0.044	0.030
OQ2	27.4	0.050	0.049

Table 3.6

Harmonic	components [dgr/hr]	Amplitude [m] monsoon	march/april	phase angle [dgr] monsoon	march/april
MSf	1.015894	0.124493	0.095797	−9.63566	74.26763
Mm	0.544375	0.052205	0.101594	65.96151	−67.9901
O1	13.94	0.066312	0.047801	77.8394	−17.2560
K1	15.04	0.162594	0.136307	1.572187	−70.6645
2MS2	27.97	0.088808	0.106064	−23.0312	−41.1398
N2	28.44	0.352001	0.188764	−58.4387	34.15695
M2	28.98	1.644839	1.585175	18.48758	69.45160
L2	29.53	0.091209	0.054354	−78.7436	56.83238
S2	30	0.678038	0.869529	2.3981	8.648096
M4	57.97	0.187162	0.183020	36.62983	62.92715
MS4	59	0.180662	0.224651	−46.8610	−13.0571
2MS6	88	0.059787	0.082733	−9.93669	81.21124
Constant:		3.507715	3.027516		

Table 3.8 Admiralty Tide Tables

Harmonic component	Amplitudes [m] Saugor	Diamond H	Calc Kidderpore	Calculated amplitudes [m] Monsoon	March/April
MSf	0.015	0.168	0.276	0.125	0.0957
Mm	0.011	0.036	0.083	0.052	0.102
O1	0.058	0.069	0.064	0.066	0.048
K1	0.151	0.153	0.124	0.163	0.136
2MS2	0.046	0.092	0.07	0.089	0.106
N2	0.272	0.291	0.201	0.352	0.189
M2	1.405	1.574	1.105	1.645	1.585
L2	0.059	0.078	0.062	0.091	0.054
S2	0.642	0.68	0.451	0.678	0.87
M4	0.027	0.229	0.222	0.187	0.183
MS4	0.023	0.215	0.198	0.181	0.225
2MS6				0.06	0.083

Table 3.7

monsoon	component [degr/hr]	amplitude [m]	inaccurate amplitude	ampl. [m] separate	inaccurate amplitude
MSf	1.015894	0.124	#	0.125	#
Mm	0.544375	0.052	#	0.052	#
O1	13.94	0.066	#	0.070	#
K1	15.04	0.163	#	0.163	#
2MS2	27.97	0.089		0.153	#
N2	28.44	0.352		0.336	
M2	28.98	1.645		1.643	
L2	29.53	0.091	#	0.079	#
S2	30	0.678		0.713	
M4	57.97	0.187		0.195	
MS4	59	0.181		0.179	
2MS6	88	0.060	#	0.059	#

march/april	component [degr/hr]	amplitude [m]	inaccurate amplitude	ampl. [m] separate	inaccurate amplitude
MSf	1.015894	0.096		0.086	#
Mm	0.544375	0.102		0.099	
O1	13.94	0.048	#	0.049	#
K1	15.04	0.136		0.136	
2MS2	27.97	0.106		0.092	
N2	28.44	0.189		0.184	
M2	28.98	1.585		1.590	
L2	29.53	0.054		0.056	
S2	30	0.870		0.872	
M4	57.97	0.183		0.169	
MS4	59	0.225		0.224	
2MS6	88	0.083	#	0.082	#

Appendix 4.1

Truncation error as a result of numerical approximation

In general

The numerical approximation of the continuity equation inevitably introduces truncation errors. The order of the inaccuracies can be examined by Taylor series. First only the space-dependent parts are discretized. Further on, the time-dependent part is treated similarly. Approximation of the continuity equation (continuous in t):

$$\left(\frac{\partial c}{\partial t}\right)_{z=(i-0.5)\Delta h} = \bar{\varepsilon}_s \left(\frac{c(i-1) - 2c(i) + c(i+1)}{(\Delta h)^2}\right) + w\left(\frac{c(i+1) - c(i-1)}{2\Delta h}\right) \qquad (1)$$

The terms on the right side of the equation represent the discretized space-dependent terms.

The first term is an approximation by a Taylor series of the second order at t=t, following from:

$$c(i-1) = c(i) - \Delta h \, \frac{\partial c(i)}{\partial z} + \frac{\Delta h^2}{2!} \, \frac{\partial^2 c(i)}{\partial z^2} - \frac{\Delta h^3}{3!} \, \frac{\partial^3 c(i)}{\partial z^3} + \frac{\Delta h^4}{4!} \, \frac{\partial^4 c(i)}{dz^4} - \;\ldots \qquad (2)$$

$$c(i+1) = c(i) + \Delta h \, \frac{\partial c(i)}{\partial z} + \frac{\Delta h^2}{2!} \, \frac{\partial^2 c(i)}{\partial z^2} + \frac{\Delta h^3}{3!} \, \frac{\partial^3 c(i)}{\partial z^3} + \frac{\Delta h^4}{4!} \, \frac{\partial^4 c(i)}{\partial z^4} + \;\ldots \qquad (3)$$

+

$$c(i+1) - 2c(i) + c(i-1) = \Delta h^2 \, \frac{\partial^2 c(i)}{\partial z^2} + \frac{2\Delta h^4}{4!} \, \frac{\partial^4 c(i)}{\partial z^4} + \;\ldots \qquad (4)$$

The originally second derivative of the concentration is numerically approximated with an error of the order $(\Delta h)^2$:

$$\frac{c(i+1)-2c(i)+c(i-1)}{\Delta h^2} = \frac{\partial^2 c(i)}{\partial z^2} + \frac{2\Delta h^2}{4!}\frac{\partial^4 c(i)}{\partial z^4} + \ \ldots \qquad (5)$$

The error of the term, that represents the influence of the fall velocity, is also an order of $(\Delta h)^2$. ***Equation (2)*** has to be subtracted from ***equation (3)*** in order to obtain the approximation of this term:

$$\frac{c_t(i+1)-c_t(i-1)}{2\ \Delta h} = \frac{\partial c_t(i)}{\partial z} + \frac{\Delta h^2}{3!.2}.\frac{\partial^3 c_t(i)}{\partial z^3} + \ \ldots \qquad (6)$$

Both formulations (5) and (6) are implemented in the mathematical equation:

$$\begin{aligned}\left(\frac{\partial c}{\partial t}\right)_{z=i} &= -\varepsilon_s \frac{\partial^2 c(i)}{\partial z^2}_{t=t} + w\frac{\partial c(i)}{\partial z}_{t=t} \\ &= \varepsilon_s \left(\frac{c(i-1)-2c(i)+c(i+1)}{(\Delta h)^2}\right) - \frac{2\Delta h^2}{4!}\frac{\partial^4 c(i)}{\partial z^4} - \ldots \\ &\quad + w\left(\frac{c(i+1)-c(i-1)}{2\Delta h}\right) - \frac{\Delta h^2}{3!.2}\frac{\partial^3 c(i)}{\partial z^3} - \ \ldots\end{aligned} \qquad (7)$$

Both errors due to the approximation of the space-dependent terms of the right side of the equation are of the second order of Δh, which means that no term is significantly inaccurate compared to the other, assuming that the third and fourth derivative of the concentration are of the same order, and both terms are fairly precise (second order error).

Next, equation (7) is discretized with respect to time. The space-dependent parts at the right hand side are evaluated at time t, therefore, no terms involving powers of Δt appear. In the left hand side, the time-dependent term,

$$\left(\frac{\partial c}{\partial t}\right)_{z=i} = \frac{c_i(t+dt) - c_i(t)}{\Delta t} \tag{8}$$

produces a first order error:

$$c_i(t+\Delta t) = c_i(t) + t\ c_i(t)' + \frac{\Delta t^2}{2!}\ c_i(t)'' + \frac{\Delta t^3}{3!}\ c_i(t)''' + \ \ldots \tag{9}$$

$$\boxed{\frac{c_i(t+\Delta t) - c_i(t)}{\Delta t} = c_i(t)' + \frac{\Delta t}{2!}\ c_i(t)'' + \frac{\Delta t^2}{3!}\ c_i(t)''' + \ \ldots} \tag{10}$$

The truncation error of the continuity equation is:

$$\boxed{-\frac{2\Delta h^2}{4!}\ \frac{\partial^4 c(i)}{\partial z^4} - \frac{\Delta h^2}{3!.2}\ \frac{\partial^3 c(i)}{\partial z^3} + \frac{\Delta t}{2!}\ c_i(t)'' + \ldots} \tag{11}$$

Consequently, the truncation error is of lower order in Δt than in Δh, although the actual magnitude of the errors depend on the values of the time step Δt, the layer thickness Δh and the derivatives at issue.

APPENDIX 4.2

VON NEUMANN THEORY

$$c_j^0 = c_0 e^{ikx_j} = c_0 e^{ij\xi} \qquad \xi = k\Delta z = \frac{2\pi\Delta z}{L}$$

$$c_j^{t+1} = c_j^t + \frac{\Delta t}{\Delta h}\left\{\bar{E}_s\left(\frac{c_{j-1}^t - 2c_j^t + c_{j+1}^t}{\Delta h}\right) + w\left(\frac{c_{j+1}^t - c_{j-1}^t}{2}\right)\right\}$$

FOR $t=0$, FOR $j=i$

$$c_j^1 = c_j^0 + \frac{\Delta t}{\Delta h}\left\{\bar{E}_s\left(\frac{c_{j-1}^0 - 2c_j^0 + c_{j+1}^0}{\Delta h}\right) + w\left(\frac{c_{j+1}^0 - c_{j-1}^0}{2}\right)\right\}$$

$$c_j^1 = c_0 e^{ij\xi} + \frac{\Delta t}{\Delta h}\left\{\bar{E}_s\left(\frac{c_0(e^{i(j-1)\xi} - 2e^{ij\xi} + e^{i(j+1)\xi})}{\Delta h}\right) + w\left(\frac{c_0(e^{i(j+1)\xi} - e^{i(j-1)\xi})}{2}\right)\right\}$$

$$c_j^1 = c_j^0\left\{1 + \frac{\Delta t \bar{E}_s}{\Delta h^2}\left(e^{-i\xi} - 2 + e^{i\xi}\right) + \frac{\Delta t w}{\Delta h 2}\left(e^{i\xi} - e^{-i\xi}\right)\right\}$$

$$e^{i\xi} = \cos\xi + i\sin\xi$$

$$c_j^1 = \left\{1 + \frac{\Delta t \bar{E}_s}{\Delta h^2}(2\cos\xi - 2) + \frac{w\Delta t}{2\Delta h}\, 2i\sin\xi\right\} c_j^0$$

STABILITY DEMAND:

$$\rho = 1 + \frac{\Delta t \bar{E}_s}{\Delta h^2}(2\cos\xi - 2) + \frac{w\Delta t}{\Delta h}\, i\sin\xi$$

$$|\rho| \leq 1 \qquad \text{FOR} \quad 0 \leq \xi \leq \pi$$

$$\left\{1 + \frac{2\Delta t \bar{E}_s}{\Delta h^2}(\cos\xi - 1)\right\}^2 + \left\{\frac{\Delta t w}{\Delta h}\sin\xi\right\}^2 \leq 1$$

ASSUME: $\alpha = \dfrac{\Delta t \bar{E}_s}{\Delta h^2} \qquad \beta = \dfrac{w\Delta t}{\Delta h}$

$$1 + 2\alpha(\cos\xi - 1) + \alpha^2(\cos\xi - 1)^2 + \beta^2(1 - \cos^2\xi) \leq 1$$

$$2\alpha(\cos\xi - 1) + \alpha^2(\cos\xi - 1)^2 + \beta^2(1 - \cos\xi)(1 + \cos\xi) \leq 0$$

DIVIDE BY: $\cos\xi - 1 \qquad (\cos\xi - 1 \leq 0 \quad \forall \quad 0 \leq \xi \leq \pi)$

$$2\alpha + \alpha^2(\cos\xi - 1) - \beta^2(1 + \cos\xi) \geq 0$$

$$(\alpha^2 - \beta^2)\cos\xi + 2\alpha - \alpha^2 - \beta^2 \geq 0$$

MINIMA / MAXIMA IF $\cos\xi = 1 \vee \cos\xi = -1$

$\cos\xi = 1$

$$\alpha^2 - \beta^2 + 2\alpha - \alpha^2 - \beta^2 \geqq 0$$

$$2\alpha - 2\beta^2 \geqq 0$$

$$\alpha - \beta^2 \geqq 0$$

$$\frac{2\Delta t\,\varepsilon_D}{\Delta h^2} \geqq \frac{\Delta t^2 w^2}{\Delta h^2}$$

$$\frac{0{,}5\,w^2 \Delta t^2}{\Delta h^2} \leqq \frac{\varepsilon_D \Delta t}{\Delta h^2}$$

$\cos\xi = -1$

$$-(\alpha^2 - \beta^2) + 2\alpha - \alpha^2 - \beta^2 \geqq 0$$

$$-2\alpha^2 + 2\alpha \geqq 0$$

$$-\alpha + 1 \geqq 0$$

$$-\alpha \geqq -1$$

$$\alpha \leqq 1$$

$$\frac{\varepsilon_D \Delta t}{\Delta h^2} \leqq 0{,}5.$$

<u>STABILITY CRITERION:</u>

$$\boxed{\frac{0{,}5\,w^2 \Delta t^2}{\Delta h^2} \leqq \frac{\varepsilon_D \Delta t}{\Delta h^2} \leqq 0{,}5}$$

Appendix 5.1

The determination of the input variables

The velocity

The velocity data obtained during the measuring campaign was adapted before it was applied. The velocity was registered every minute by the velocity meter. This data fluctuated considerably, so it was smoothed out by a programme, that calculates the average of a number of measurements for every time step. Here, the velocity is averaged over 11 time steps. This amount was chosen after comparing the results of several amounts of time steps.

Selection of location

The data of location III-B is selected for calibration after comparison with the measured concentration at the other locations. Initially, the intension was to use I-A as reference location. The sampling at this location, however, did not succeed as well as at III-B. Location II-A is not typical of the whole area, because the depth is smaller than at the other locations and the bar causes divergent flow conditions. The programme has been applied for III-B and was improved upon. Later on, it can be applied to the other locations. This was not accomplished within the framework of this study due to lack of time.

The value of the critical shear stress velocity and the fall velocity depend on parameters that are typical of both material and hydraulic conditions. These parameters need to be determined first. The following scheme shows the mutual dependence of the parameters.

w depends on:
- D
- ρ_s
- ρ
- ν

v_{*cr} depends on:
- ν
- g
- Δ
- D

v_* depends on:
- v
- ρ
- C
    - * h
    - * r = bottom roughness
        - D

The determination process in chronological order:

$$\left.\begin{array}{l} -\ D \\ -\ \rho(\text{Temperature, Salinity}) \\ -\ \nu(\text{Temperature}) \end{array}\right\} \qquad \left.\begin{array}{c} r \\ w \\ \\ + \\ \\ h \end{array}\right\} \qquad \begin{array}{c} C \\ \\ v_* \end{array}$$

Grain sizes

The characteristic grain sizes are determined by both an external geotechnical laboratory and within the framework of this study. The latter method was more inaccurate, but both results are shown in ***table 2.11***.

In I-B, both methods have the same D_{90} and only the laboratory gives information about the smaller D's. The results in II-B are comparable, though the grain sizes, determined by the laboratory are smaller. They are assumed to be the most reliable. The grain sizes in III-B show large differences between both methods and the laboratory grain sizes are larger than the others.

It is, however, not necessary that the suspended sediment is connected to the material at the bed, for it can be wash load. The grain size of the wash load is assumed to be smaller than the bed material, for else it would not be in suspension, but settle on the bed.

The diameters applied to determine the parameters are the D_{30} and the D_{50} as lower and upper boundaries. As the grain sizes in I-A are coarser than in I-B and the material in II-A is finer than in II-B, estimations of upper and lower boundaries are based on the information of the sieving in the framework of this study.

The density

The measurements with the density float gave densities of about 998 up to 1000 kg/m^3. The density of the water samples were measured for both the samples at the water surface and the samples taken near the bed. There was no significant difference between the densities on both levels in the vertical at all three locations over a period of one tidal cycle. It is assumed that no density currents occur in this area. The relative density is still 1.65.

The kinematic viscosity

The kinematic viscosity depends on the temperature of the water in the Hooghly River, which is approximately 30 ^{0}C (measured by a thermometer, contained in the velocity meters). According to the Hydro compendium of the Hydraulic Laboratory, the kinematic viscosity is $0.8*10^{-6}$ m^2/s.

The fall velocity

The fall velocity can be determined in several ways, according to:

-1 an empirical formula [van der Velden, 1989]

$$\log(\frac{1}{w}) = 0.4949(\log D_{50})^2 + 2.4113(\log D_{50}) + 3.7394$$

-2 the formula following from the equilibrium between the downward submerged weight of the particle and the upward drag force [van der Velden, 1989]

$$w = \frac{(\rho_s - \rho) g D^2}{18 \rho \nu}$$

-3 graphical results of research, done by Komar and Reimers [Dyer, 1986]

-4 fall velocity, sieve diameters relation [V146]

-5 a graphical representation of fall velocity [Raudkivi, 1967]

The results are shown in ***table 5.1.1***. The fall velocity according to the formulae and graphs are determined for varying temperatures. A higher temperature results in a lower viscosity, which eventuates a higher fall velocity. There are only two determinations of the fall velocities with a temperature of 30 ^{0}C. The other calculations show the variance in values for the fall velocity. The kinematic viscosity is 0.8 m^2/s for a temperature of 30^{0}C ; for a temperature of 21^{0}C, it is 1.0 m^2/s. The fall velocities determined according to number 4 are read from a graph with double logarithmic scales, and therefore, the results are not accurate.

The critical shear stress velocity

The critical shear stress velocity is not determined from the Shields curves [Hydro compendium and Graf, W.H., 1971], because the flow velocity that is needed to determine shear stress velocity of the Reynolds number is constantly fluctuating. The formula:

$$v_* = \sqrt{gRI} \tag{14}$$

cannot be used to determine the shear stress velocity, because the slope is not constant in time and no situation of equilibrium is reached.

The Shields curve from van der Velden [1989] must be extrapolated for grain diameters smaller than 125 μm. For D = 95 μm, the critical shear stress is 0.0011 m/s, after extrapolation. The values at the axes of the Shields curve are:

$$Re = \frac{v_* D}{\nu} \qquad \psi = \frac{\tau_{cr}}{(\rho_s - \rho) g D}$$

Ψ is the Shields parameter.

The empirical formula, given below, has been derived from laboratory tests [Dyer, 1985], is applied to determine the critical shear stress velocity. However, the values of the results are low compared to the used values in de Reus [1979].

$$u_*^{\frac{5}{2}} = 0.06g(\frac{\rho_s - \rho}{\rho})\nu^{\frac{1}{2}}D^{\frac{1}{2}}$$

The critical shear stress velocities are in ***table 5.1.2***.

The Chézy coefficient

The shear stress velocity is calculated by the formula:

$$v_* = \frac{v\sqrt{g}}{C}$$

Therefore, the value of the Chézy coefficient needs to be known. The Chézy coefficient is determined, using the formula of White-Colebrook:

$$C = 18\log(\frac{12h}{r})$$

There are a number of relations between the bottom roughness, r, and the characteristic grain sizes. Five of them are used to calculate the Chézy coefficient for different water levels (h). The values of these Chézy coefficients appear to be very high, from 92 $m^{½}/s$ up to 122 $m^{½}/s$. (See ***table 5.1.3***).

The water levels

Initially, the water level was held constant during the run of the computer programme at the level of 6.9 m for III-B. The average water level was determined from the registrations. The registrations of the Oil jetty were applied, and corrected for the depth by fitting the water level curve of the Oil Jetty to depth registrations made by the echo-sounder. For III-B, a phase lag was determined in that same manner. Although the registration station of Balari Bar is closer to location III-B, its registration was not used, because the lower part of the curve is deformed as a result of the reflection of the water caused by the batthymetry of the location.

The number of layers and the time step

The number of layers, m, and the time step, dt, follow from the stability demands, according to ***section 4.6***. At first, a time step of 3 seconds was chosen and 7 layers were used in the calculations.

The initial concentration

The first concentration, determined from the sampling, is the initial concentration. This concentration is determined by means of a sample at a depth of about 1.30 m, whereas the concentration has to be on a depth of 0.5 m, schematizing the water depth in 7 layers of about 1 m. The initial concentration is converted to this depth by using the equation of a equilibrium vertical concentration distribution. For III-B, the initial concentration is 2030 mg/l.

The diffusion coefficient

The diffusion coefficient is calculated according the formula:

$$\varepsilon_s = \alpha v_* h$$

The value of α is 0.067, as the diffusion coefficient is averaged over the depth, but as in de Reus [1979], the value of α can be varied.

The remainder of the input variables

The period between the successive slack waters on 01/08/91 is 12 hrs 32 min, in seconds: 45120 s. This value is used for the tidal period in the model. The ending time T_{end} of the calculation is not crucial for the calculation, but is set on 45120 s. The velocities have to be put in the input file under "table" over this time period and the initial velocity is the first velocity from "table". The interval time nt between the velocities is 60 seconds. The Von Karman coefficient κ is taken constant at 0.4.

Appendix 5.2

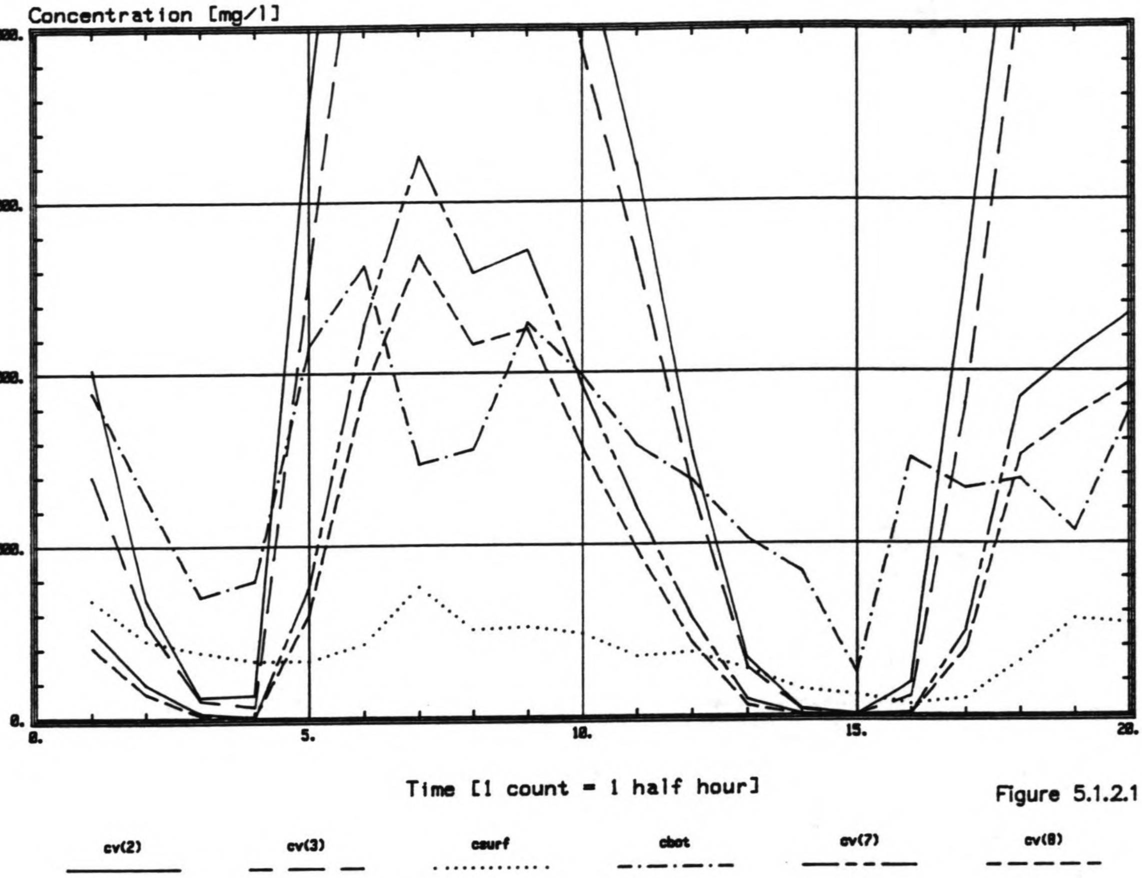

Figure 5.1.2.1

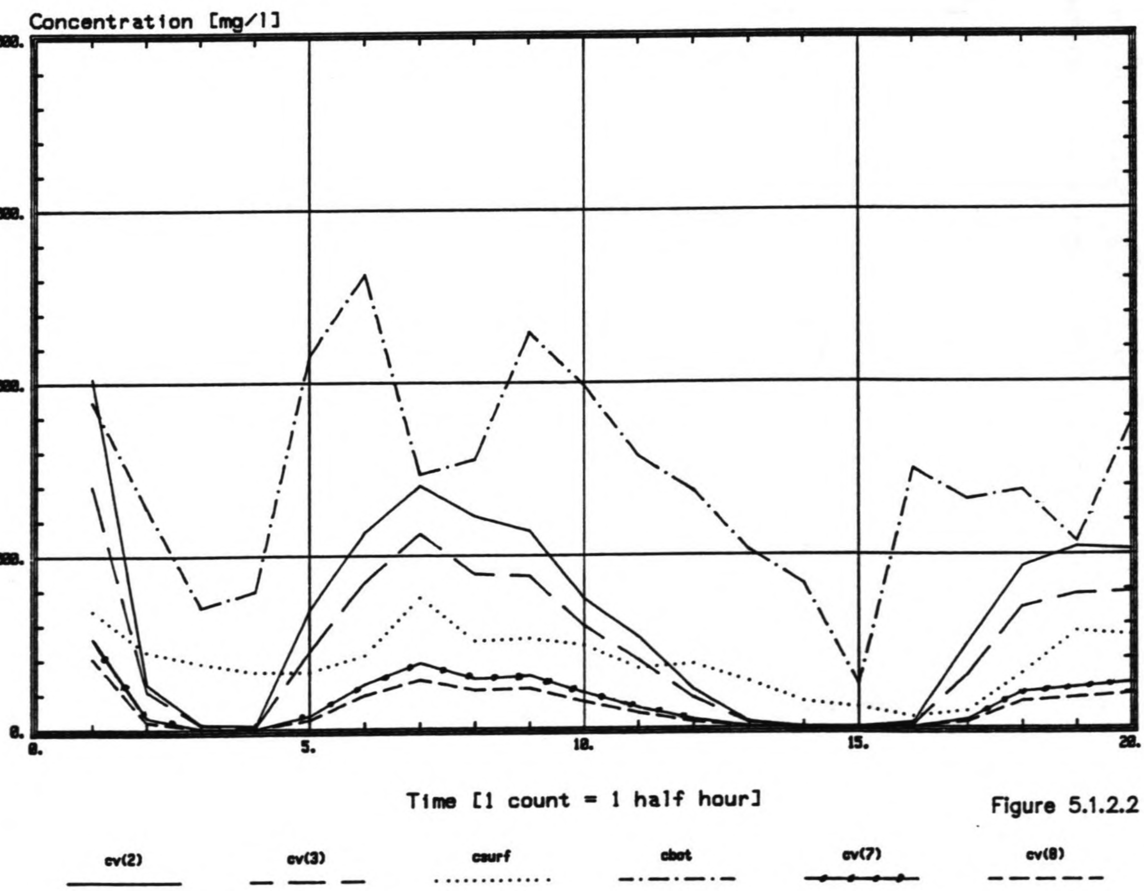

Figure 5.1.2.2

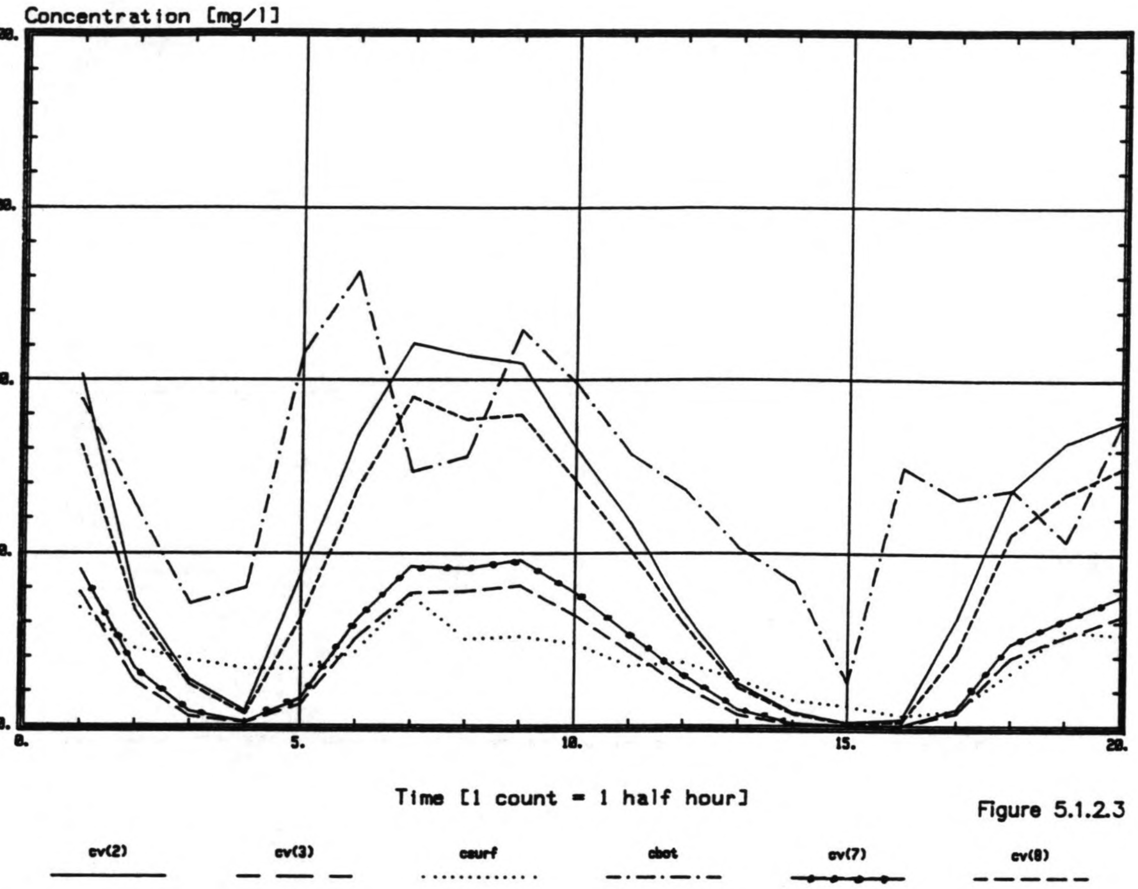

Figure 5.1.2.3

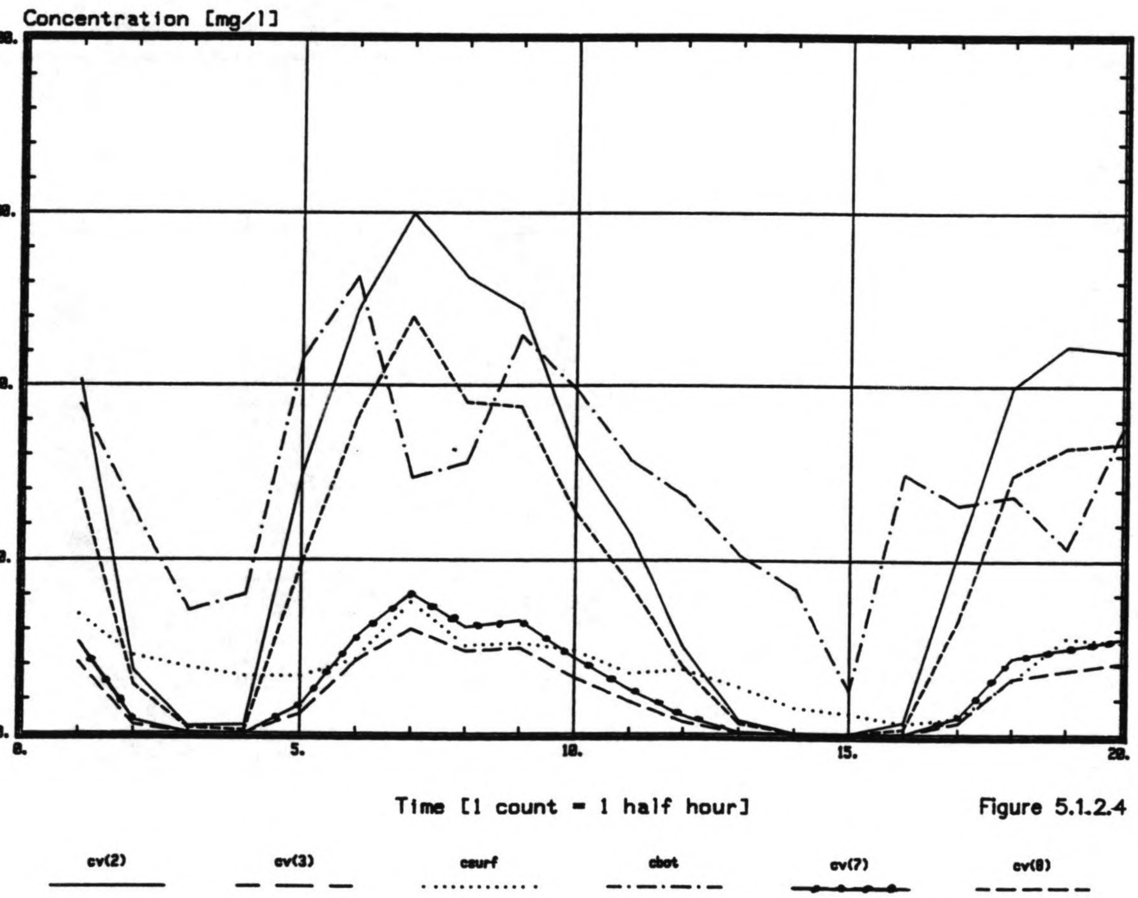

Figure 5.1.2.4

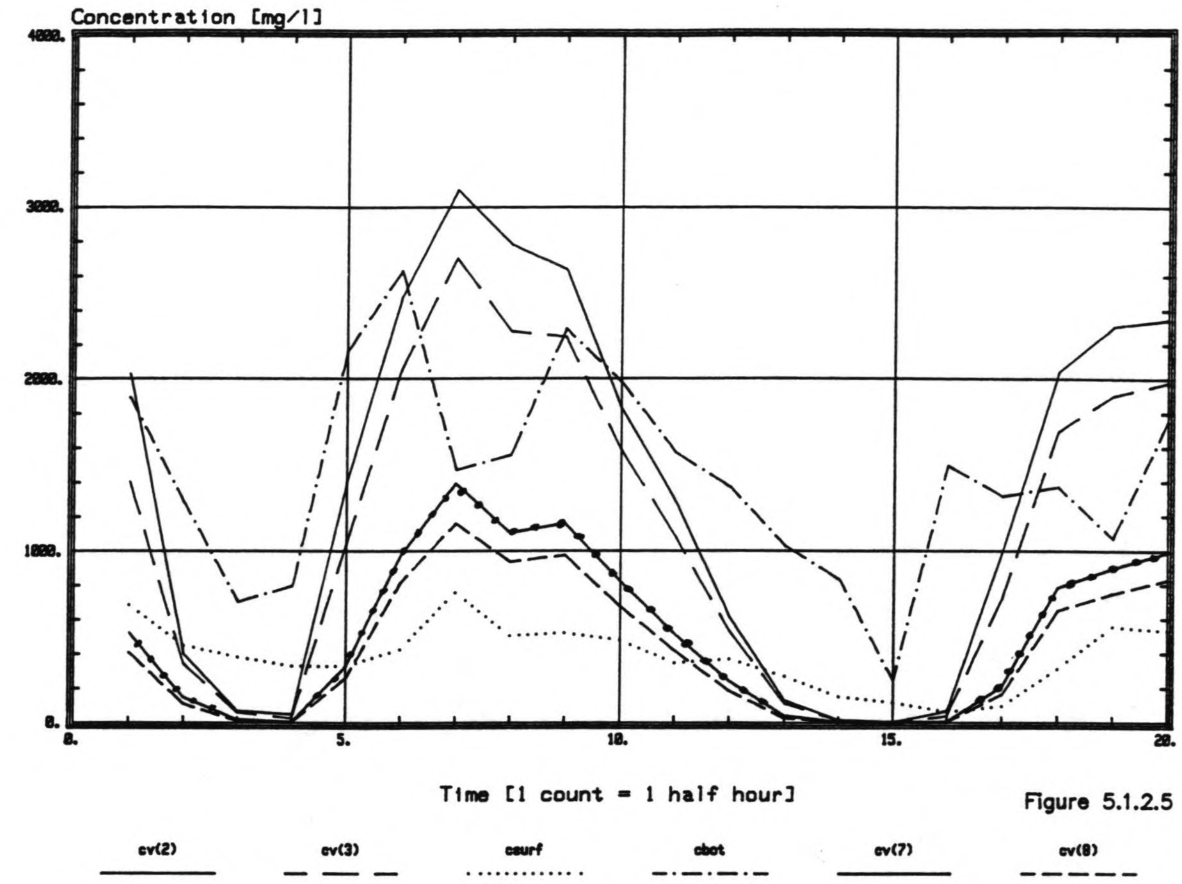

Figure 5.1.2.5

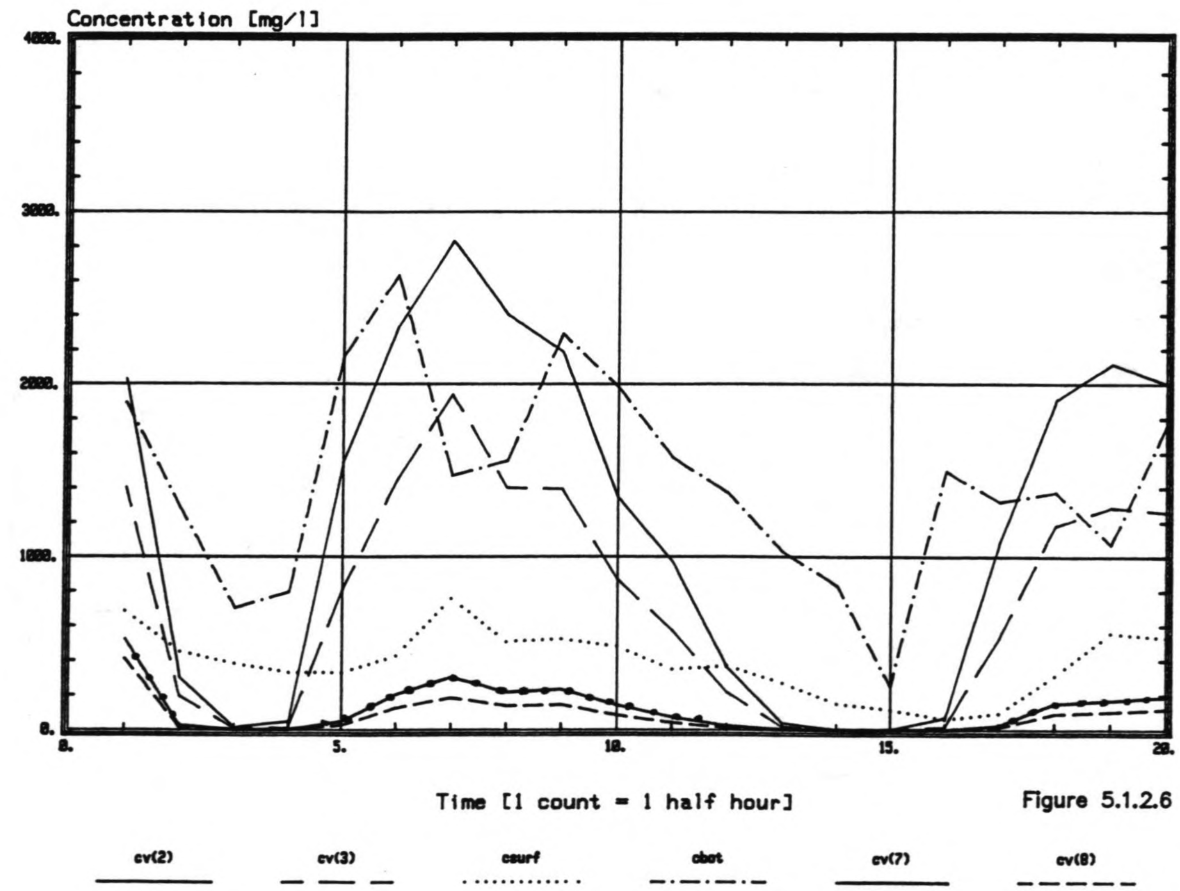

Figure 5.1.2.6

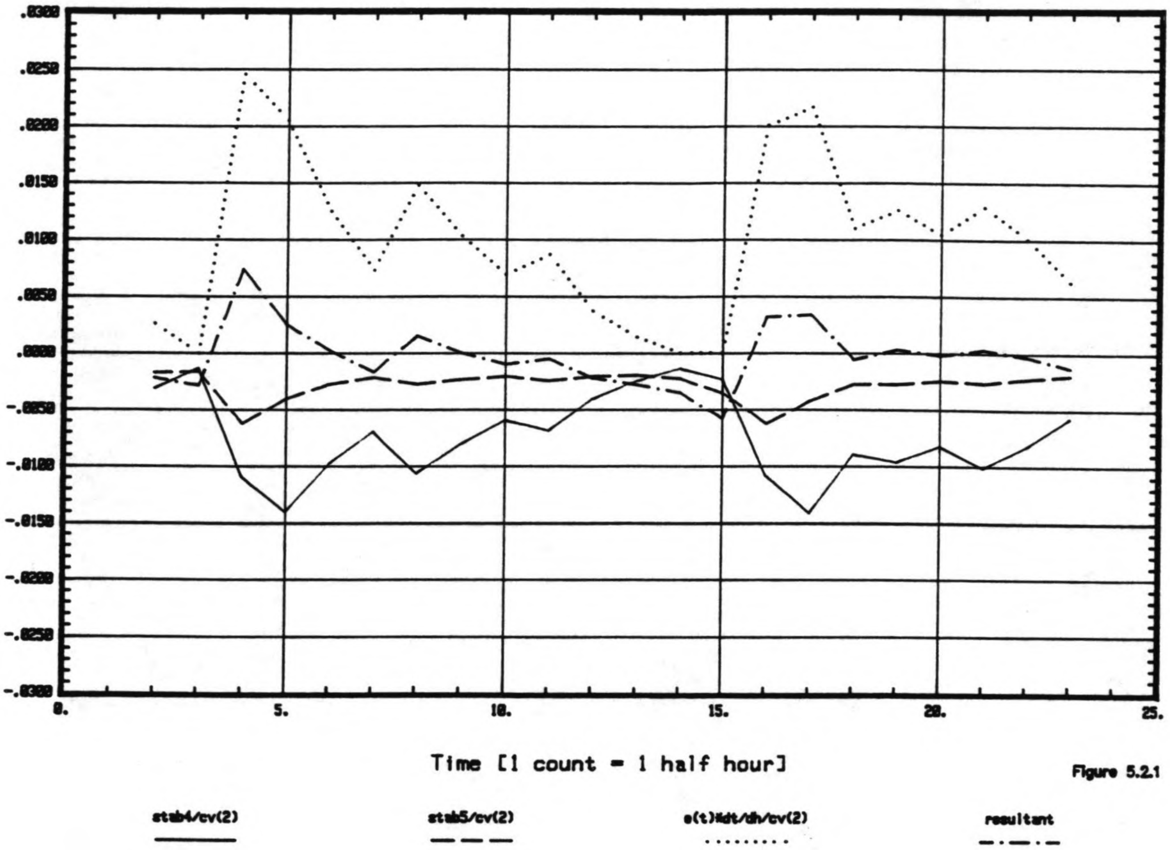

Figure 5.2.1

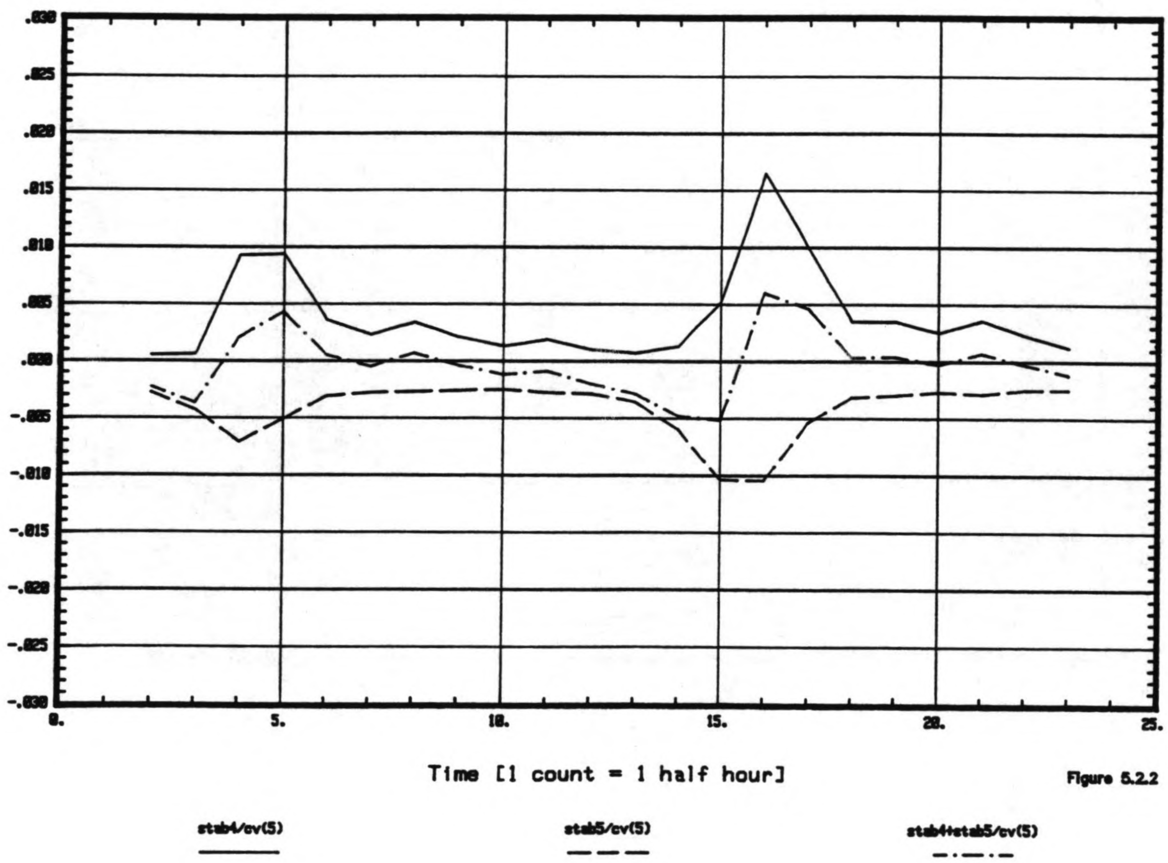

Figure 5.2.2

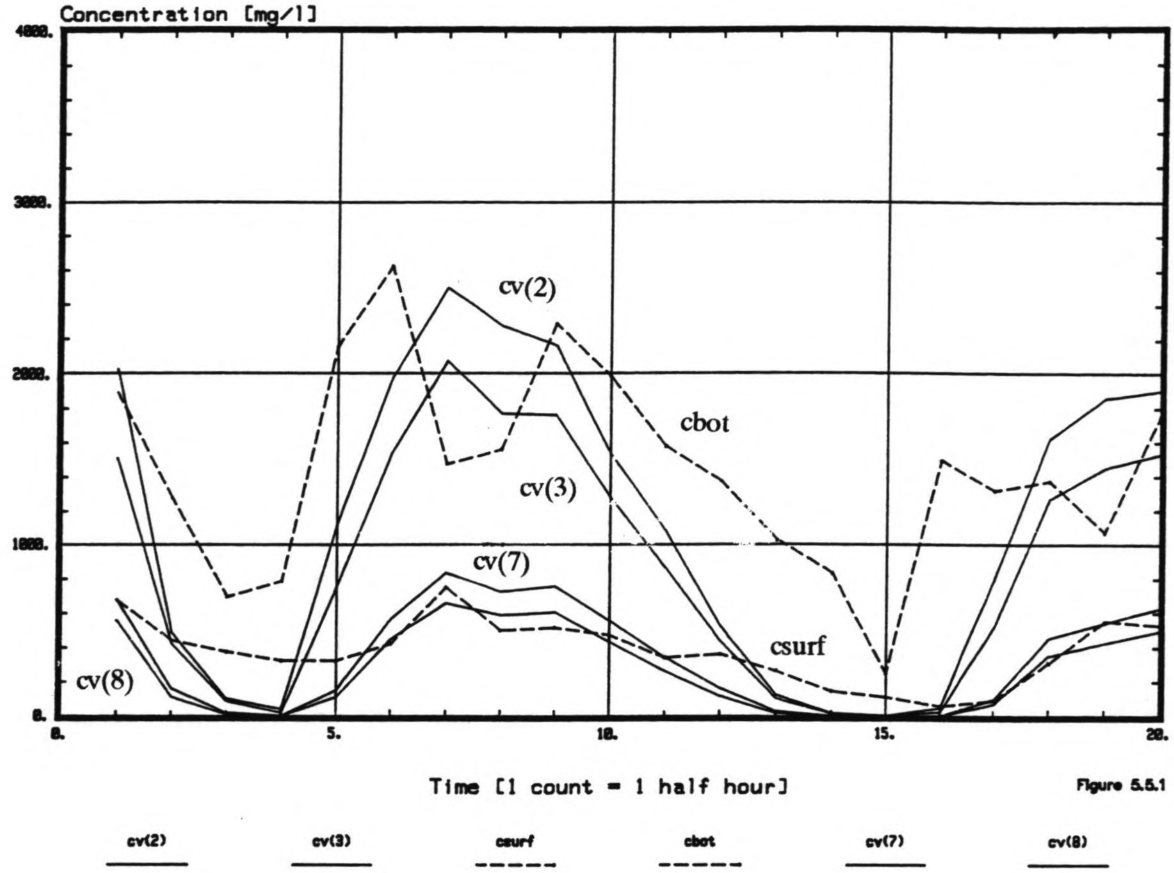

Figure 5.5.1

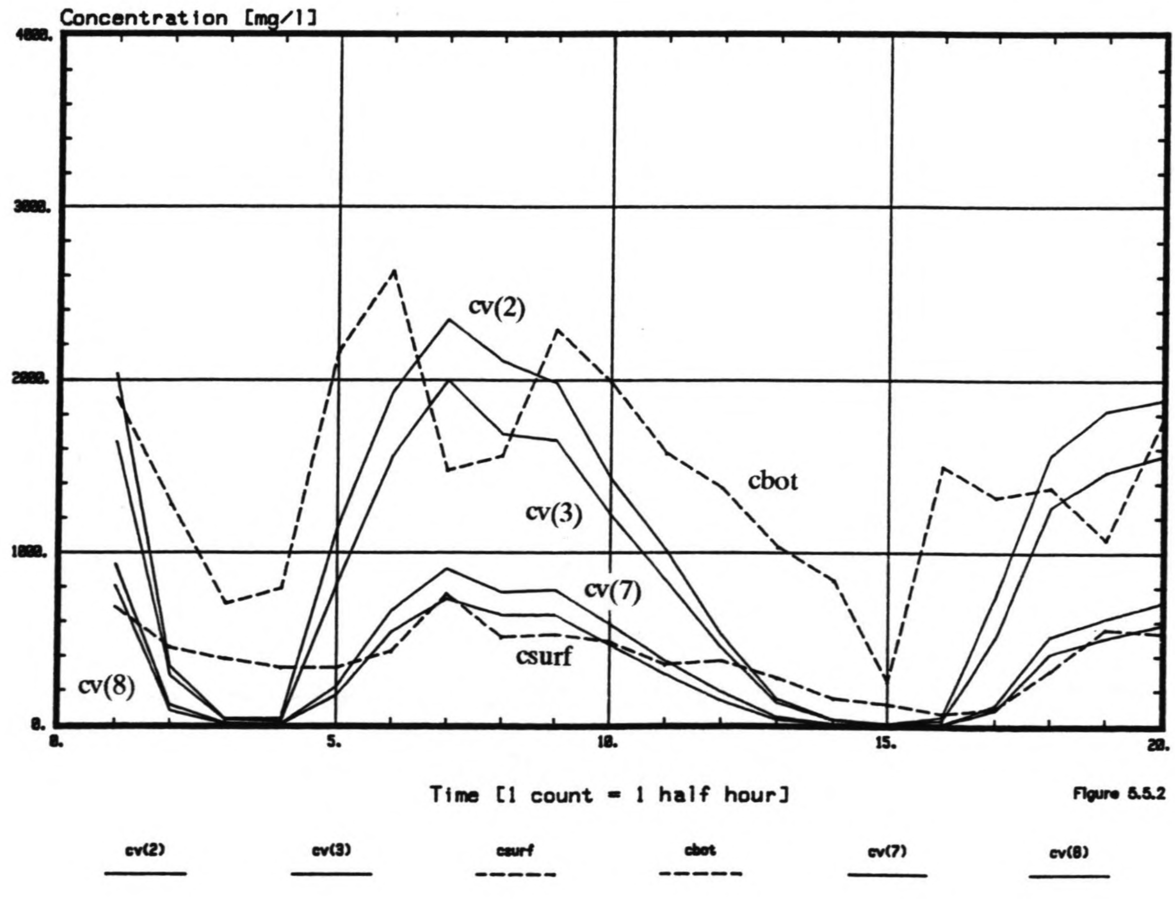

Figure 5.5.2

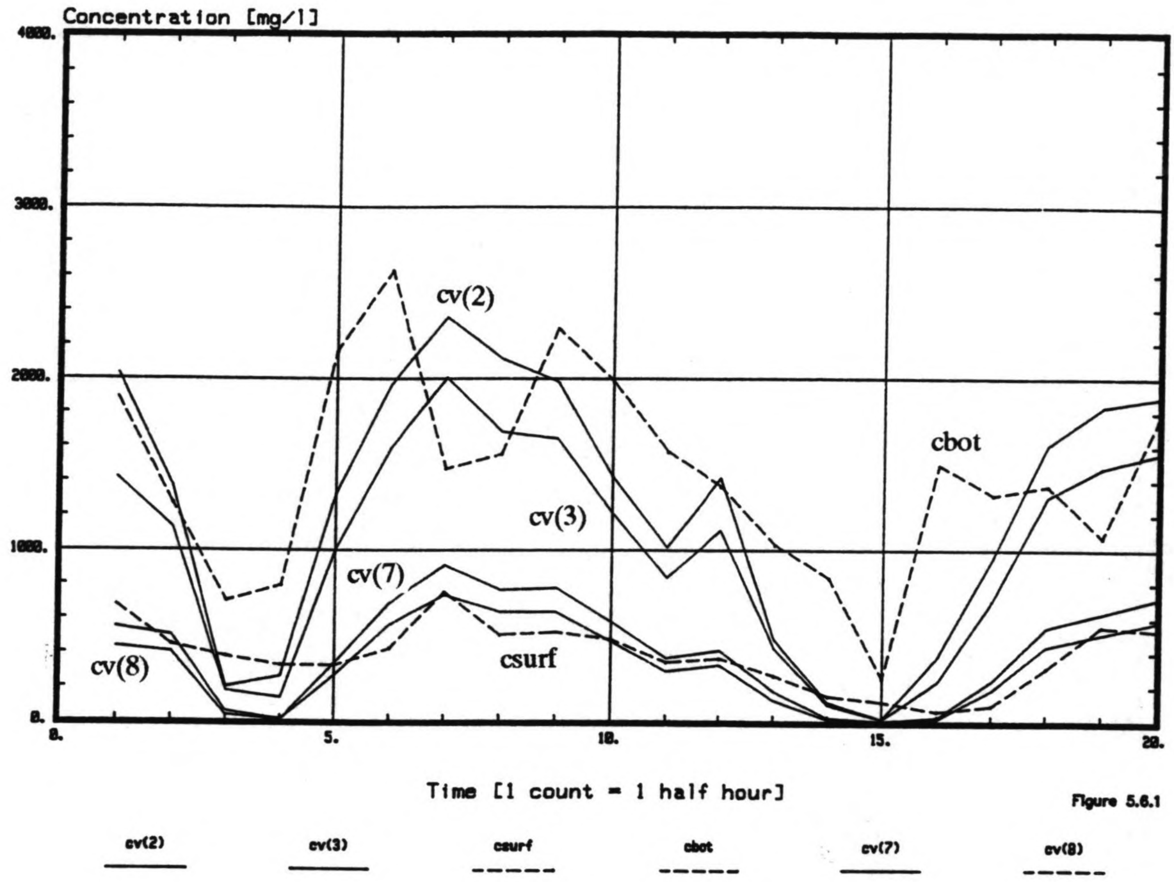

Figure 5.6.1

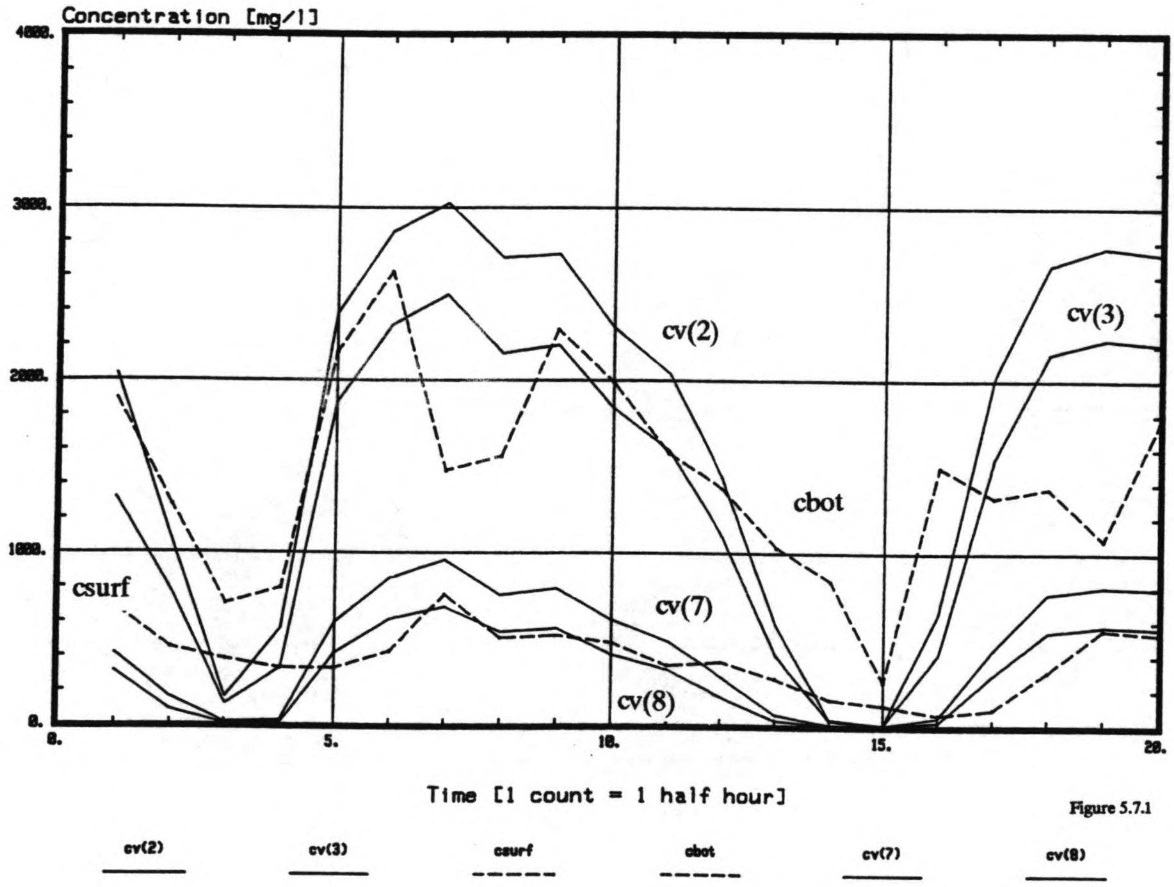

Figure 5.7.1

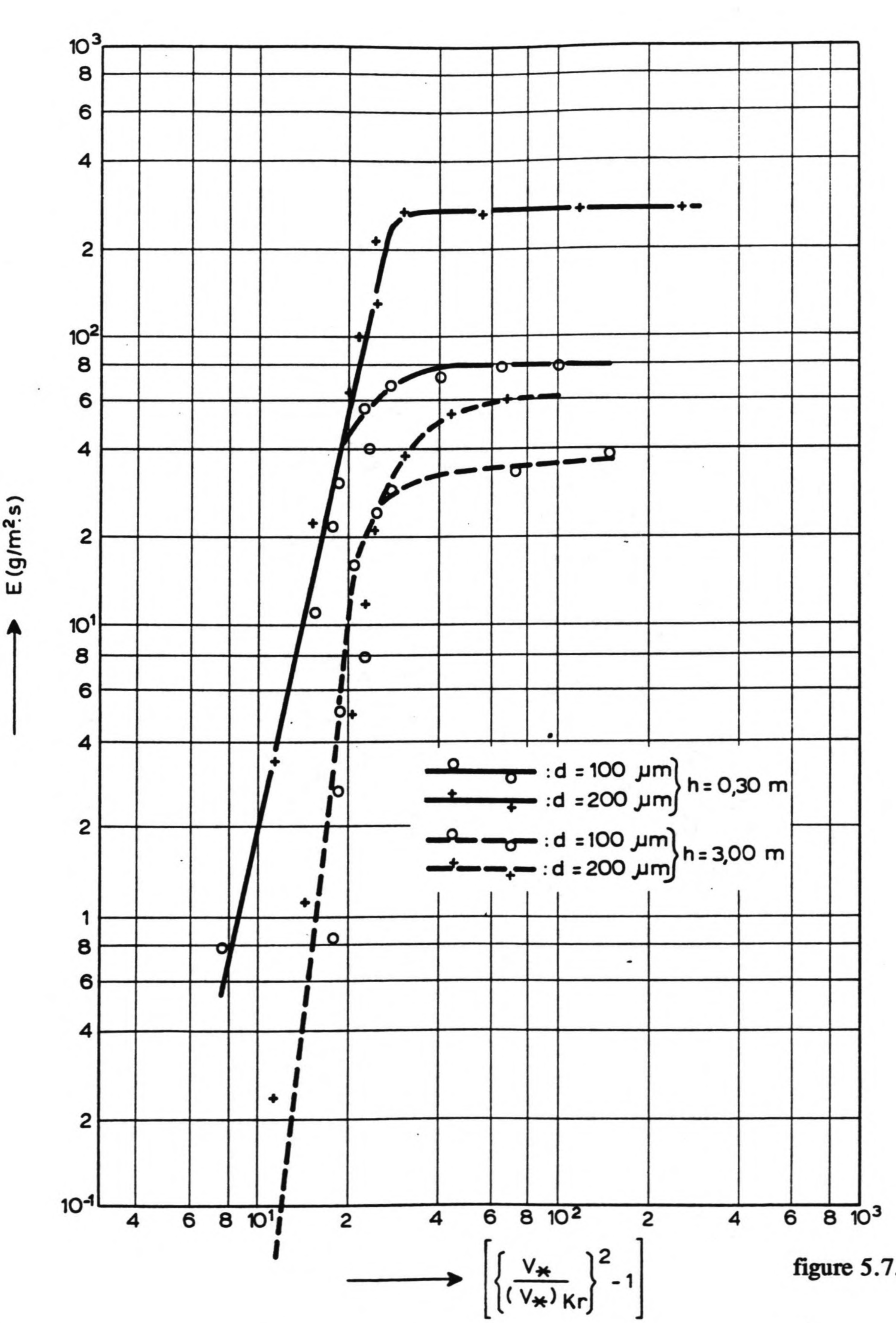

E (g/m²·s)
10^3
8
6
4
2
10^2
10^1
1
10^{-1}
4
6
8
10^1
2
10^2
10^3
: d = 100 µm
: d = 200 µm
h = 0,30 m
h = 3,00 m
$\left[\left\{\frac{V_*}{(V_*)_{Kr}}\right\}^2 - 1\right]$

figure 5.7.2

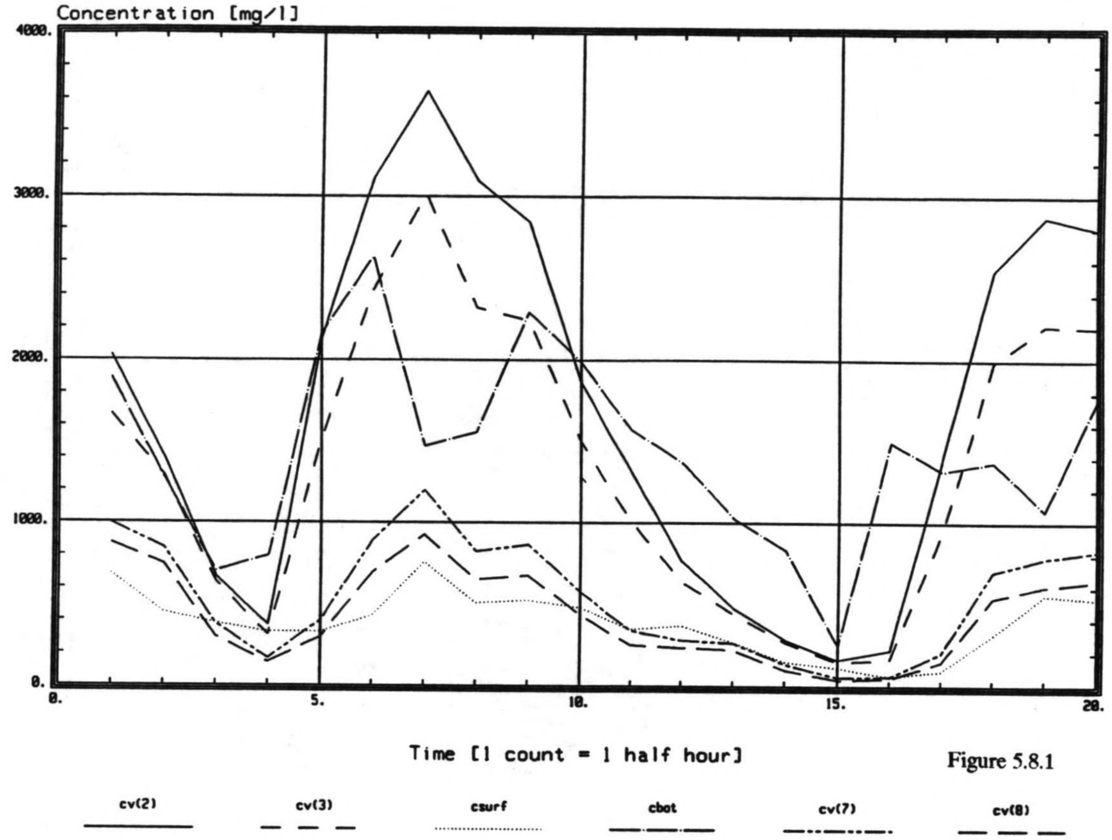

Concentration [mg/l]
4000.
3000.
2000.
1000.
0.
0.
5.
10.
15.
20.
Time [1 count = 1 half hour]
cv(2)
cv(3)
csurf
cbot
cv(7)
cv(8)

Figure 5.8.1

Appendix 5.3

Table 5.1.1 Fall velocities in m/s

Diameter [mu]	(1)	(2a)	(2b)	(3a)	(3b)	(4a)	(4b)	(5)
10	0.00009			0.00007	0.00010			
20	0.00046			0.00027	0.00037			0.00036
25	0.00075			0.00042	0.00056			0.00061
45	0.00246	0.00227	0.00182	0.00131	0.00174			0.00210
50	0.00300	0.00281	0.00225	0.00161	0.00213			0.00240
55	0.00357	0.00340	0.00272	0.00193	0.00255			0.00400
60	0.00417	0.00404	0.00323	0.00229	0.00301	0.00490	0.00400	0.00460
70	0.00544	0.00550	0.00440	0.00300	0.00390			0.00650
85	0.00750	0.00811	0.00649	0.00480	0.00590			0.00890
90	0.00823	0.00910	0.00728	0.00500	0.00650	0.00920	0.00761	0.00910
95	0.00900	0.01013	0.00811	0.00630	0.00780			0.01130
105	0.01047	0.01238	0.00990	0.00673	0.00878	0.01200	0.00972	
110		0.01359	0.01087	0.00737	0.00960	0.01250	0.01047	0.01220
115		0.01485	0.01188	0.00803	0.01045	0.01300	0.01123	
120		0.01617	0.01294	0.00871	0.01134	0.01400	0.01202	
135		0.02047	0.01637	0.01094	0.01420	0.01700	0.01449	
155		0.02698	0.02158	0.01428	0.01850	0.02000	0.01804	0.01520

(1) empirical relation — 18 degr Celcius
(2) formula [van der Velden] a) nu = 0.8e−6 — 30 degr Celsius
b) nu = 1.0e−6 — 20 degr Celsius
(3) graph of Komar and Reimers — 20 degr Celsius
shape factor: 0.7, 1
(4) graph [V146] — 20 degr Celsius
(5) graph [Raudkivi] — 30 degr Celsius

Table 5.1.2 shear stress velocities in m/s

Diameter [mu]	vstcr (a)	vstcr (b)	vstcr [Reus]
50	0.0082	0.0086	0.014
55	0.0084	0.0088	
60	0.0085	0.0089	
70	0.0088	0.0092	
85	0.0092	0.0096	
90	0.0093	0.0097	
95	0.0094	0.0098	0.01
105	0.0095	0.0100	
110	0.0096	0.0101	
115	0.0097	0.0102	
120	0.0098	0.0102	
135	0.0100	0.0105	
155	0.0103	0.0108	
115	0.0097	0.0102	
120	0.0098	0.0102	
135	0.0100	0.0105	
155	0.0103	0.0108	

Table 5.1.3 Chezy coefficients in $m^{0.5}/s$

I−B

formula	I−B	D(char)	h=5.5 m	h=7 m	h=8.5 m
(1)	1.40E−05	1.75E−05	118	120	122
(2)	3.80E−05	3.80E−05	112	114	116
(3)	3.80E−05	7.60E−05	107	109	110
(4)	8.90E−05	2.23E−04	98	100	102
(5)	8.90E−05	2.67E−04	97	99	100

II−B

formula	II−B	D(char)	h=3 m	h=6 m	
(1)	1.17E−04	1.46E−04	97	102	
(2)	1.47E−04	1.47E−04	97	102	
(3)	1.47E−04	2.94E−04	92	97	
(4)	1.95E−04	4.88E−04	88	93	
(5)	1.95E−04	5.85E−04	86	92	

III−B

formula	III−B	D(char)	h=5 m	h=7 m	h=8.8 m
(1)	7.80E−05	9.75E−05	104	107	109
(2)	1.13E−04	1.13E−04	103	106	017
(3)	1.13E−04	2.26E−04	98	100	102
(4)	1.45E−04	3.63E−04	94	97	98
(5)	1.45E−04	4.35E−04	93	95	97

	Characteristic grain diameter	Formula:
(1) = Ackers−White	D35	r = 1.25 D35
(2) = Einstein	D65	r = D65
(3) = Engelund Hansen	D65	r = 2 D65
(4) = Kamphuis	D90	r = 2.5 D90
(5) = van Rijn	D90	r = 3 D90

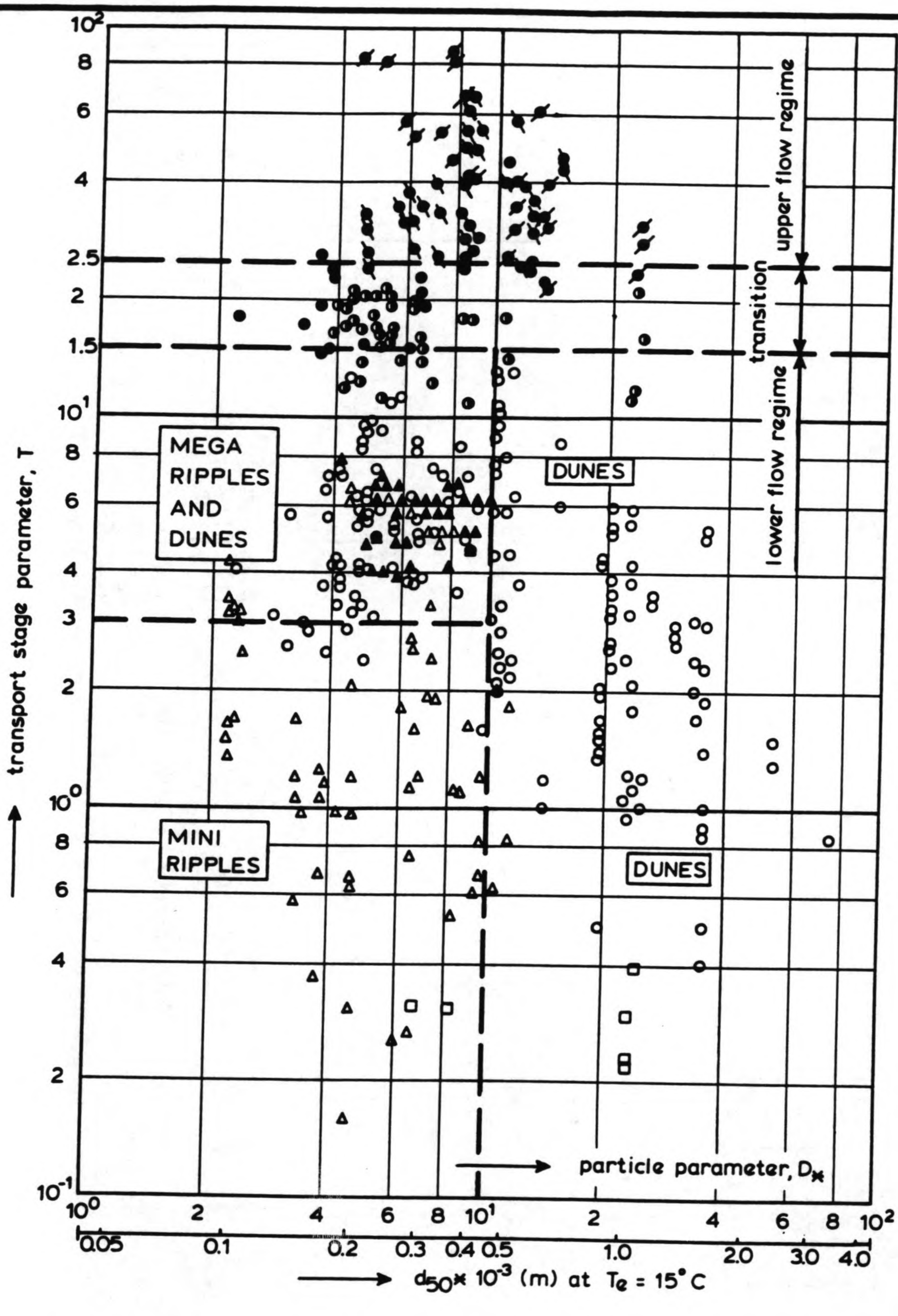

□	plane bed (no motion)	◐	washed-out dunes (transition)
△	miniripples	●	plane bed
▲	megaripples and dunes	⌀	anti-dunes (standing waves)
o	dunes	◕	anti-dunes (breaking waves)

BED-FORM CLASSIFICATION DIAGRAM
FOR UNIDIRECTIONAL FLOW, VAN RIJN

DELFT HYDRAULICS | H 461 | FIG. 1.

Appendix 5.4

The determination of the Chézy coefficient with ripples

The formulae of van Rijn are applied in order to take ripples into account in the determination of the Chézy coefficient. They are described below:

A dimensionless bed-shear stress parameter T is appointed:

$$T=\frac{\theta'-\theta_{cr}}{\theta_{cr}}$$

in which:

$$\theta'=\frac{u_*^2}{\Delta g D_{50}}$$

$$\theta_{cr}=0.24\,D_*^{-1}$$

$$D_*=[\frac{\Delta g}{\nu^2}]^{\frac{1}{3}}D_{50}$$

There are three ways to determine what kind of bed form is existing under certain conditions:

-1 the bed form classification diagram for unidirectional flow, van Rijn (***figure 1***)

-2 the bed form classification diagram for unidirectional flow, van den Berg (***figure 2***) both drawn from van Rijn [1990]

-3 examine the Froude number: this is only useful under upper regime conditions. In III-B, only lower regime conditions occur, as the Froude number does not exceed Fr=1.

ad 1 The particle parameter D_*, for III-B the D_* is 2.8, and the D_{50} (95 μm) are plotted against the transport stage parameter T. The limits, where the bed form changes into another form, are given in ***table 5.4.1***. The mega ripples are assumed to be disappeared for T $\approx$ 10.

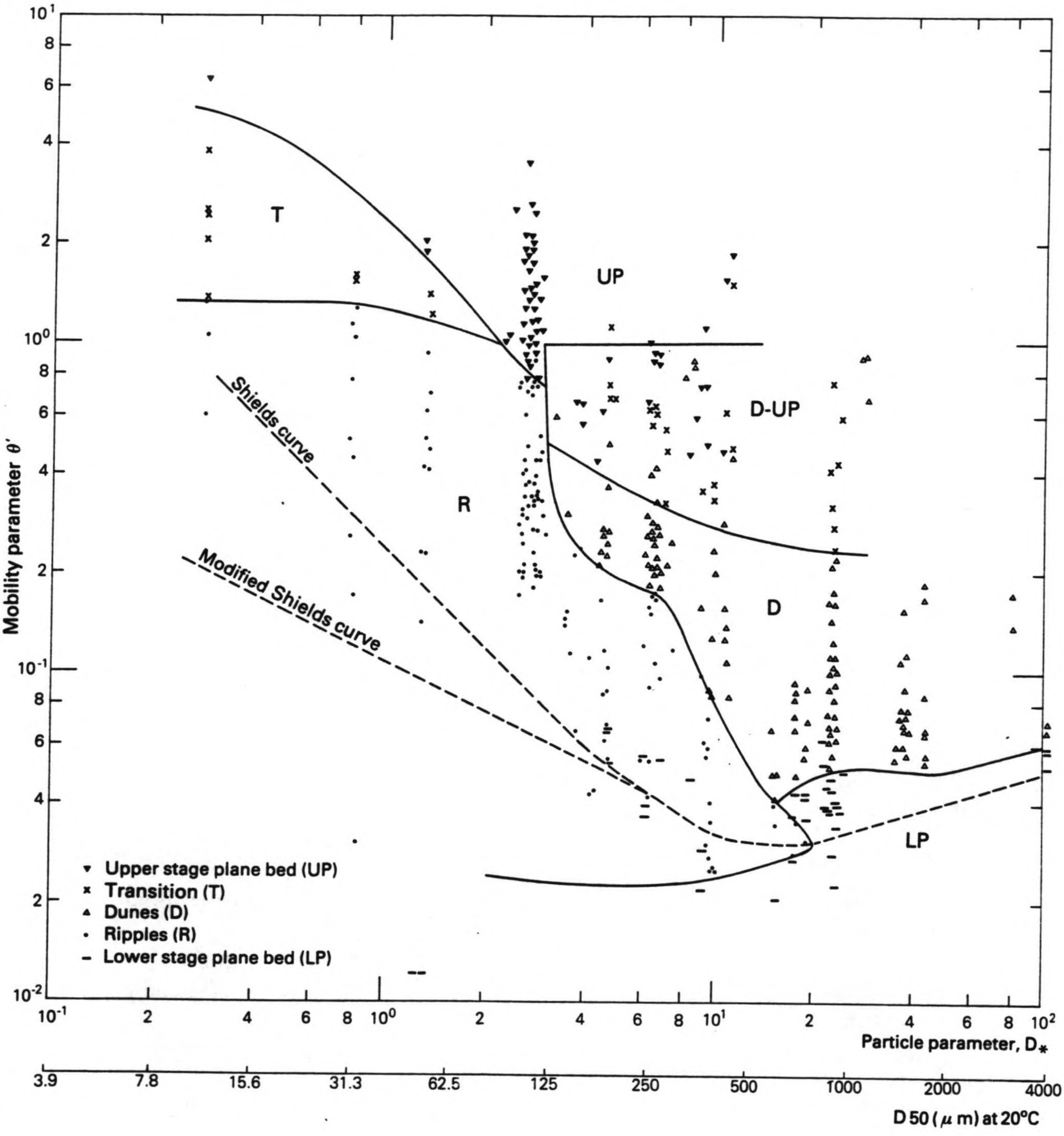

BED FORM CLASSIFICATION DIAGRAM FOR UNIDIRECTIONAL FLOW, VAN DEN BERG (1989), FLUME DATA

DELFT HYDRAULICS	H 461	FIG. **2.**

Table 5.4.1

parameter T	bed form
T < 3	mini ripples
3 < T < 15	mega ripples and dunes
15 < T < 25	washed out dunes
25 < T	anti dunes

ad 2 The particle parameter D_* and the D_{50} are plotted against the mobility parameter θ. According to this curve, only ripples and upper stage plane bed occur in III-B. The limits for different bed forms according to this diagram are in ***table 5.4.2***.

Table 5.4.2

mobility parameter θ'	bed form
θ < 0.06 to 0.07	no movement
0.07 < θ < 0.8 to 1	ripples
0.8 to 1 > θ	upper stage plane bed

According to the latter diagram, it is assumed that only ripples occur under low velocities and that the bed (partly) washed out for higher velocities. Yalin [van Rijn, 1990] reports estimations of heights and lengths for mini ripples. The range of these estimations is large, so the results are not accurate. The Chézy coefficient for mega ripples is determined by estimating the ripple height and length according to the formulae of van Rijn [1990].